NPL
National Physical Laboratory

Report

NPL REPORT
DEPC-MPE 033

Environment Assisted Cracking of Turbine Blade Steels – A Review

Shengqi Zhou

NOT RESTRICTED

MARCH 2007

dti
National Measurement System

National Physical Laboratory | Hampton Road | Teddington | Middlesex | United Kingdom | TW11 0LW

Switchboard 020 8977 3222 | **NPL Helpline** 020 8943 6880 | **Fax** 020 8943 6458 | **www.npl.co.uk**

dti

The DTI drives our ambition of 'prosperity for all' by working to create the best environment for business success in the UK. We help people and companies become more productive by promoting enterprise, innovation and creativity.

We champion UK business at home and abroad. We invest heavily in world-class science and technology. We protect the rights of working people and consumers. And we stand up for fair and open markets in the UK, Europe and the world.

The National Physical Laboratory is operated on behalf of the DTI by NPL Management Limited, a wholly owned subsidiary of Serco Group plc

Environment Assisted Cracking of Turbine Blade Steels – A Review

Shengqi Zhou
Engineering and Process Control Division

ABSTRACT

This short report provides an overview of environment assisted cracking (EAC) of blade steels. The effect of material composition, chloride concentration and temperature on pitting is assessed. Critical pitting potential measurement using a potentiodynamic scan shows that the threshold chloride concentration for pitting of a 12% Cr steel in the absence of dynamic stain is in excess of 500 ppm, much higher than that in the condensate on the steam turbine under normal operating conditions. There is a significant effect of environment on the fatigue strength, with no evidence of a fatigue limit in aggressive environments, e.g., concentrated NaCl and NaOH solutions. In less aggressive environments pitting may still influence the development of cracks but only acting in concert with fatigue loading, the latter assisting initial pit development either by film breakdown or microcrevice formation at inclusions and sustaining propagation of the subsequent pit. In this case, a fatigue limit is still observed because pitting is contingent upon fatigue loading but it is lower than that in air.

There is generally little effect of environment on the growth rate of fatigue cracks under high frequency cyclic loading. However, in aggressive environments, such as NaCl solution, the threshold stress intensity factor range for fatigue cracking can be reduced relative to air, probably associated with dissolution of microstructural barriers to crack propagation. There is a marked effect of environment on the crack growth rate under load waveforms simulating two shifting operating conditions. Measurements of stress corrosion cracking (SCC) velocities are sparse. Significant crack growth rates have been reported but seem tied in with steels of high S and P impurity levels or very aggressive environments. In more relevant environments with modern steels the growth rate is very low, typically about 0.2 mm/y.

Keywords: Steam turbines, blade steels, pitting, fatigue, environment assisted cracking

ISSN 1744-0262

National Physical Laboratory
Hampton Road, Teddington, Middlesex, TW11 0LW

We gratefully acknowledge the financial support of the UK Department of
Trade and Industry (National Measurement System Policy Unit)

Approved on behalf of the Managing Director, NPL,
by Dr M G Gee, Knowledge Leader, Materials Performance Team
authorised by Director, Engineering and Process Control Division

CONTENTS

1. INTRODUCTION

Failures from environment assisted cracking (EAC) of steam turbine blades, discs and rotors have been a concern in the power industry. Despite worldwide effort, occasional problems still arise. The major challenge is to predict more reliably the conditions under which cracking is likely and, for those conditions, the evolution of crack size with time so that non-destructive testing may be used in a focused manner and informed decisions made about inspection intervals and remnant life.

Failures from stress corrosion cracking (SCC) of steam turbine blade steels are less frequent compared to disc steels. Consequently, studies on SCC of blade steels are not as extensive as for the disc steels and most of the work has focused on corrosion fatigue (CF).

This brief review is supplementary to the previous comprehensive review on EAC of steam turbine disc steels[1]. The objective is to review critically existing data on pitting, crack initiation and crack growth in blade steels and the effect of material properties (strength level, composition), environmental variables (pH, oxygen, chloride and carbon dioxide concentrations), temperature and stress on EAC.

2. CRACKING IN SERVICE

2.1 LOCATIONS

For fossil fired power stations, most turbine blade failures have occurred in the last few rows of the low pressure (LP) turbine as it is in this region that the steam starts to condense[2.] EAC has also occurred on high pressure (HP) turbine blades where condensation forms in Magnox and PWR stations but as the blades are smaller and the stresses are lower it is less common.

2.2 MATERIALS

It has been stated[3] that the most common blade materials used in steam turbines at fossil fired and nuclear power plants are martensitic steels containing 11%-13% Cr and a variety of secondary alloying elements depending on the manufacturer, with the yield strength ranging from 600 MPa to 800 MPa. However, both Westinghouse and GEC have used blade steels with yield strength starting at 550 MPa and GEC have used higher strength steels (FV566) in the range of 700 MPa to 1000 MPa[4]. Other steels, such as high nitrogen 12% Cr steels, precipitation hardened stainless steels (e.g. PH 17-4), duplex stainless steels and Titanium alloys (e.g. Ti-6Al-4V) have also been used as blade material in steam turbines[3,5-7] to improve the mechanical strength and/or the corrosion resistance. However, this review focuses on EAC of the more commonly used martensitic blade steels.

2.3 STRESS

Blades are subjected to static stresses, which result predominantly from centrifugal loads with a design limit stress of 50% of the yield stress or less[8,9], and to transient stresses caused by start up/shut down cycles. In addition to these static or quasi-static loads are superimposed high frequency cyclic loads due to vibrations or steam bending. The amplitudes of the high frequency cyclic stresses are often unknown and depend on assumptions[3], although they are expected to be low, about 0.5% of the yield stress and no more than 1% under normal operating conditions[3]. Accordingly, for most applications, high frequency fatigue failure would be uncommon.

2.4 TEMPERATURE

The temperature of blades at locations where EAC occurs varies from station to station, depending on the turbine design and operating conditions[10]. For instance, the temperature at which first condensation occurs ranges from about 90 ºC in low pressure turbines (LP) for the typical fossil fired plant, to 280 ºC in high pressure turbines (HP) for a PWR station. However, it should be noted that the transient temperature on the blade surface during start up/shut down may be very different from that under normal operation conditions. Thus, last row LP blades normally operate at about 40 ºC but can reach 150 ºC during start up, shut down, no-load or light load running due to windage effects (friction due to air)[11].

2.5 IMPURITIES

The various studies of deposition of corrosive salts on steam turbines have been well documented in a number of reviews[12-14]. Over 150 chemical compounds have been identified in millimetre thick deposits with concentrations ranging from a few ppm by weight of deposit to almost 100% of the deposit[14]. It was thought that the main cause for EAC of the turbine discs and blades was due to the formation of highly concentrated solution in the early droplets nucleated around the particles. Therefore, early studies had focused on CF and SCC of blade steels in concentrated corrosive solutions, such as NaCl and NaOH.

However, more recent studies[10,15,16] suggest that concentrated solutions are not a reflection of the solution chemistry of condensates in the region of relevance to EAC. A comprehensive review[10] on water chemistry of condensates on the turbine surface has been conducted recently and key conclusions can be summarised as follows:

- Calculations based on thermodynamics have shown that the content of inorganic impurities in the liquid film is predicted to be 100 times higher than that in the steam, assuming that formation of the liquid film commences at a moisture level of 1%.

- In-situ measurements using a model power plant at the Moscow Electricity Institute (MEI)[16] show that the concentration factor (the ratio between the impurity concentration in the early condensate and in the inlet steam) is between 10 and 50, i.e. less than that calculated by assuming that all impurities are partitioned in the liquid phase and that the moisture level is 1% or less.

- The chloride concentration measured for the liquid film was more variable, in the range of 50 to 1000 times higher than that in the inlet steam. Evaporation was suggested as the possible cause of the presence of the much higher chloride concentration in the liquid films compared to that in the early condensates.

- Due to the partitioning of oxygen between the steam and liquid phase, the oxygen in the liquid film and early condensate should always be less than 1 ppb under normal operating conditions. Under abnormal and transient conditions (air leakage, forced condensation, off-load), oxygen levels of up to several ppm may be present in the condensates.

These studies suggest that condensate chemistry under normal operation could be typified by relatively low concentrations of salts, e.g. 300 ppb Cl^- + 300 ppb SO_4^{2-} or 1.5 ppm Cl^- solutions although the details will vary from plant to plant.

3. LABORATORY TESTING

3.1 PIT INITIATION AND GROWTH

EAC of blade steel often initiates at pit sites which act as stress raisers, especially for low and moderate strength steels[5,17-20]. Pits can promote crack development, in general, by acting as stress concentrators, by creating a local solution chemistry conducive to cracking and by removing impediments to hydrogen ingress through dissolution of oxide film[21].

Systematic measurement of critical pitting potentials for a wide range of steels, including conventional 12% Cr blade steels, the high nitrogen alloys and the precipitation hardening steels, was carried out by Lopez-Cacicedo and McIntyre[8], using potentiodynamic scanning at a rate of 0.5 mV/s. The tests were conducted in aerated 0.02 M NaCl solution at 23 ºC and 90 ºC. (To compare data from different sources, it is worthwhile to note that 0.01 M [Cl^-] is equal to 355 ppm Cl^- and 1 ppm Cl^- is equivalent to 2.8×10^{-5} M [Cl^-]). As shown in Figure 1, an empirical relationship was established between critical pitting (breakdown) potential, E_b, and the contents of major elements in the steels:

$$E_b, \text{mV (SCE)} = 54.6\,[\%Cr + 3(\%Mo + \%W)] - 855 \qquad (1)$$

Williams and McMurray[22] measured E_b for two steam turbine steels, FV566 containing 11% Cr and FV520B containing 13.5% Cr by mass, using potentiodynamic polarisation at a sweep rate of 0.5 mV/s. The critical pitting potentials in various concentrations of NaCl solution at 25 ºC to 100 °C are shown in Figure 2. The following relationship between E_b and chloride concentration was obtained from a linear fit:

$$E_b = A + B \log_{10}[Cl^-] \qquad (2)$$

where A and B are constants. The values of A and B for the 11% Cr and 13.5% Cr steam turbine blade steels at different temperatures are listed in Table 1.

It can be seen that the pitting resistance of the steels increased significantly with increasing Cr content from 11% to 13.5%, the values for 13.5% Cr steel being about 0.25 V higher than that of 11% Cr steel.

Williams and McMurray[22] reported that under open circuit a 13.5% Cr steel showed no evidence of pitting when immersed in aerated electrolyte at 20 °C for up to 4 days, even when [Cl^-] was 5 mol/l. Under the same conditions, stable pits commenced on an 11% Cr steel within 1 h of immersion at [Cl^-] ≥ 1 mol/l (35500 ppm).

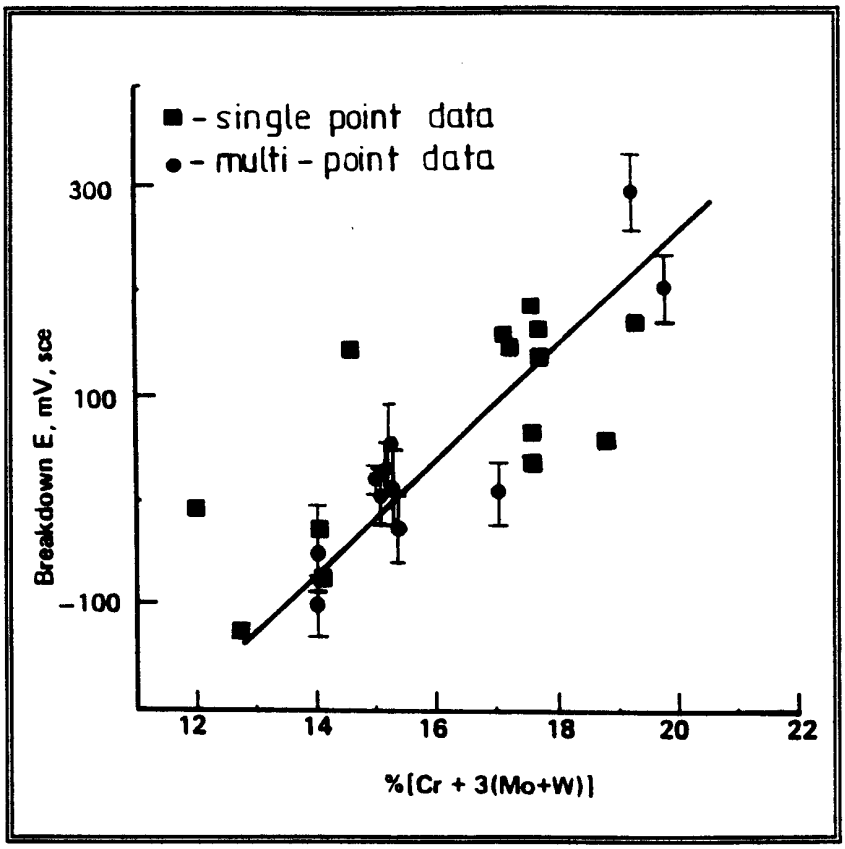

Figure 1. Correlation between breakdown potential of blade steels and %[Cr + 3(Mo +W)] in 0.02 M NaCl solution[8].

Table 1 A and B parameters (from Eqn 2) for the 11% Cr and 13.5% Cr steam turbine blade steels as a function of temperature in chloride-containing solutions[8].

Temperature (°C)	A /V (SCE)		B / V/Decade	
	11Cr	13.5Cr	11Cr	13.5Cr
25	0.011	0.277	-0.142	-0.146
40	0.003	0.247	-0.139	0.130
55	-0.059	0.176	-0.124	-0.142
70	-0.146	0.114	-0.148	0.153
85	-0.205	0.068	-0.138	-0.131
100	-0.258	0.008	-0.145	-0.141

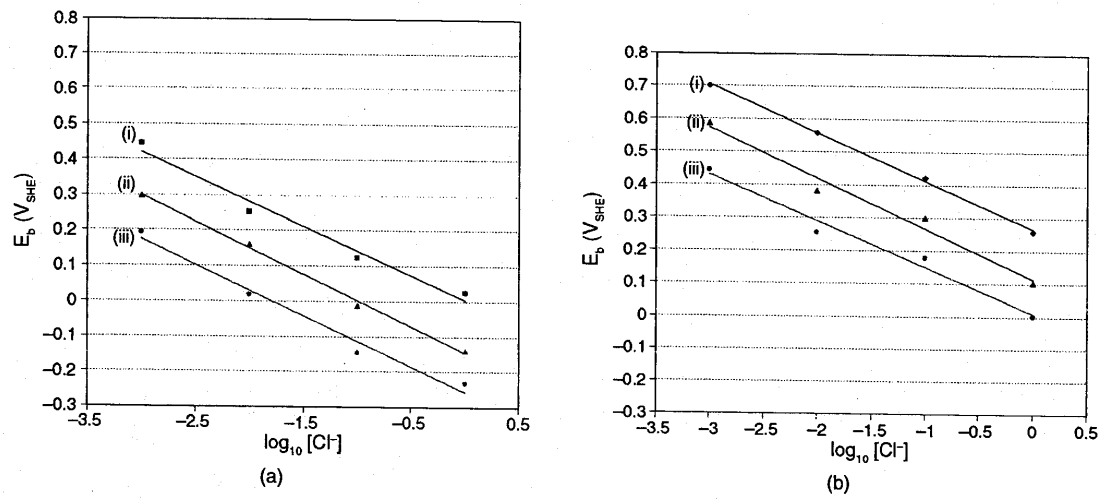

Figure 2. Pitting diagrams showing the variation of E_b with [Cl^-] in deaerated aqueous NaCl solution for (a) 11% Cr and (b) 13.5% Cr alloy. Results are shown for temperatures of: (i) 25 °C, (ii) 70 °C, and (iii) 100 °C[22].

The E_b of a blade steel (FV566) containing 12% Cr by mass was measured in deaerated water containing various Cl^- contents at 90 ºC, using the potentiodynamic scanning technique at a sweep rate of 1 mV/s[23]. The measured E_b values are shown in Figure 3 as a function of chloride concentrations, together with the corrosion potential in various aerated chloride solutions (1.8 ppm O_2). The corrosion potential was measured after the specimen had been exposed to the solution for 24 h. It can be seen that pitting is unlikely until the chloride concentration reaches about 500 ppm at which concentration E_b is only about 50 mV more positive than the corrosion potential. However, it should be pointed out that the critical pitting/film breakdown potential is only indicative and cannot be directly used to identify whether a steel of interest in a given environment will suffer from pitting corrosion, as it is scan rate dependent. Any change of surface condition, such as surface roughness/surface defects or induced surface residual stress in the steel, may also have a significant effect on the critical pitting/film breakdown potential. Furthermore, the critical pitting/film breakdown potential is expected to be reduced for steels under dynamic strain[24]. Nevertheless, it seems that in the absence of dynamic strain pitting is not likely in the water chemistry relevant to steam turbine applications, such as 300 ppb, 1.5 ppm and 35 ppm Cl^- solution. However, as dynamic strain is always present in the turbine blades, further studies are required to evaluate the impact of dynamic strain on the critical pitting conditions.

For comparison, the E_b of two blade steels at 90 ºC extrapolated from equations derived by William and McMurray[22] is plotted as a function of chloride concentration in Figure 3. It appears that there is good agreement between the three sets of data with respect to the chloride concentration dependence of the critical pitting potential.

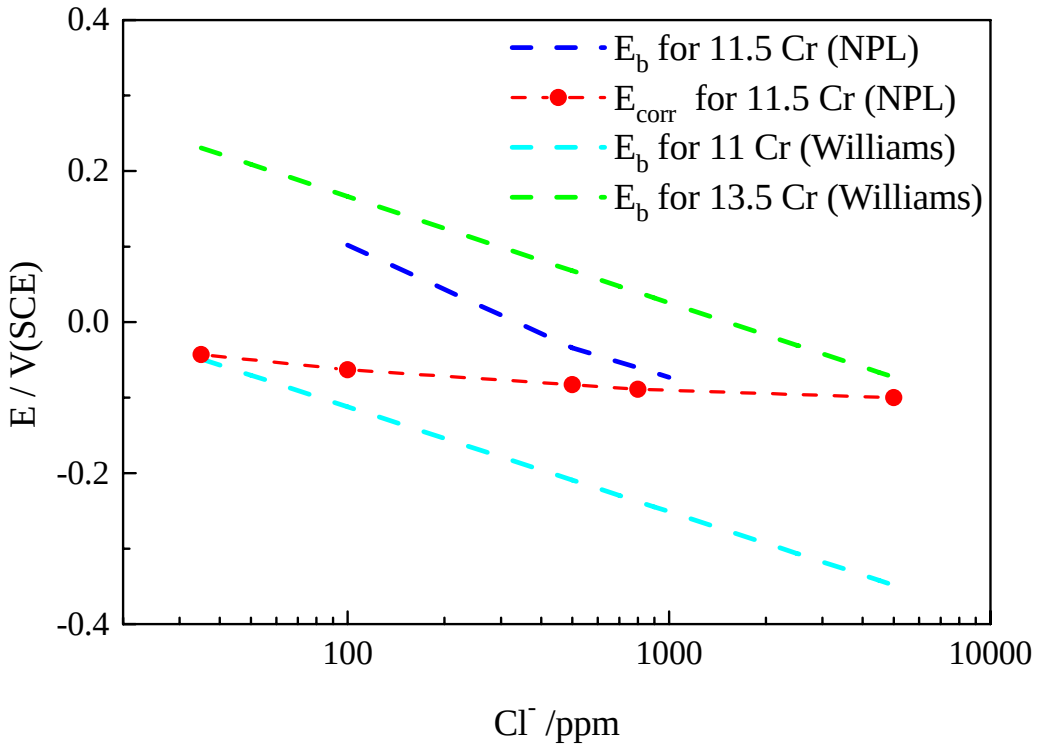

Figure 3. The critical pitting/film breakdown potential of the blade steels measured in deaerated solution as a function of chloride content. Also shown is the corrosion potential of the 12% Cr blade steel measured in aerated Cl^- solutions at 90 °C[23].

Shalaby et al[20] examined the surface appearance of fatigue specimens of a 12% Cr steel (Type 403 SS) tested in various concentrations of H_2O, NaOH, NaCl, Na_2SO_4, Na_3PO_4 and Na_4SiO_4 at 100 ºC. The fatigue tests were conducted using the rotating bending method (stress ratio, R = -1) at a frequency of 1.5 Hz. Tests were conducted first in air and then in Cl^- solutions to determine the fatigue limit. Subsequently, separate tests were performed at a stress amplitude of 448 MPa to investigate the fatigue initiation morphology in various environments. These tests were interrupted for microscopic examination at ~ 50% and 75% of the average fatigue life. The exposed side surfaces and the fractured surfaces were examined using optical and scanning electron microscopy (SEM). The finding are summarised in Table 2. Pits were observed in all NaCl solutions except in 0.01 M at pH 10 and cracks initiated from macropits except in 1.0 M at pH 2. Pits were also observed in 0.01 M and 1 M Na_2SO_4 solutions at pH 7 and pH 10 but the transition from pits to cracks only occurred in 1 M Na_2SO_4 solutions. No pitting occurred in other environments.

Table 2 Modes and characteristics of fatigue crack initiation in Type 403 SS in various environments[20].

Solution	Conc. (M)	pH	Mode	Comments
air	N/A	N/A	(1)+2	High density of long narrow cracks associated with inclusions and debonded zones
H_2O	N/A	N/A	1	Medium density of long narrow cracks
NaOH	~0.0001	10	1	Medium density of long wide cracks
	~0.01	12	(1)+2	High density of long narrow cracks
	~1.0	14	1	Medium density of long narrow cracks
NaCl	0.01	2	(4)+3	Very low density of long narrow cracks linking micropits
	0.01	7	(3)+1	Very low density of long narrow cracks initiating at macropits
	0.01	10	1	High density of short wide cracks (no pits)
	1.0	2	(4)+3	No cracks observed at 75% fatigue life. some micropits
	1.0	7	(3)+1	Very low density of long narrow cracks initiating at macropits
	1.0	10	(3)+1	
Na_2SO_4	0.01	2	4	No cracks or pits observed at 75% of fatigue life. Very low density of short narrow cracks, macropits developed at later stage
	0.01	7	(1)+3	Very low density of short narrow cracks, macropits developed at later stage
	0.01	10	(1)+2+3	Very low density of short wide cracks, macropits developed at later stage
	1.0	2	4	Same as pH = 2, $[Na_2SO_4]$ = 0.01
	1.0	7	(1)+3	Very low density of long narrow cracks transitioning macropits
	1.0	10	(1)+3	Very low density of short wide cracks, micropits developed at later stage
Na_3PO_4	0.01	2	(1)+2	High density of long narrow cracks associated with inclusions and debonded zones
	0.01	7	(1)+2	Medium density of short wide cracks
	0.01	10	(1)+2	High density of long narrow crack
	1.0	2	(1)+2	High density of long narrow cracks associated with inclusions and debonded zones
	1.0	7	(1)+2	
	1.0	10	(1)+2	
Na_4SiO_4	1.0	10	1	Low density of long narrow cracks

Note: 1. intrusion-extrusion microcracks; 2. inclusions; 3. pitting; 4. general corrosion (emergent boundary etching); and ( ), dominant mode. Very low density ≤ 75 cracks/cm^2, low density ≤ 150 cracks/cm^2, medium density ~ 300 cracks/cm^2, high density ≥ 450 cracks/cm^2. Short crack ≤ 150 μm, long crack ≥ 300 μm, narrow crack ≤ 0.5 μm, wide crack ≥1.5 μm, micropits ≤ 30 μm diam, macropits ≥ 60 μm diam.

Pits were also observed by Ebara et al[17] in 3% NaCl at 60 ºC and 80 ºC as well as in 3×10^{-4} % (3 ppm) NaCl solutions at 80 ºC. However, the test at 3×10^{-4} % NaCl solution was conducted by dripping the solution on to the specimen at a flow rate of 2-5 ml/min. It was not specified whether there was formation of any scale or salt deposits on the specimens due to evaporation, which would result in much higher local chloride

concentrations. Nevertheless, the authors quoted that others[25] at a different laboratory also reported micropits of about 10 μm deep on 13% Cr steel in 1 ppm NaCl solution at 150 ºC. Pits were also observed in specimens tested in 40% NaOH + 3.5% NaCl and 14.4% $Na_{2.8}H_{0.2}PO_4$ solutions. A surprising result is that the depth of pits was roughly constant at 10-20 μm, regardless of variation of NaCl concentration and the magnitude of cyclic stress, which in turn affects the test duration (time to failure). The authors did not give an explanation for the apparent independence of pit depth on the environments and test durations but it is possible that these were non-propagating pits due to the dissolution of inclusions under dynamic strain in fatigue tests.

The evolution of pit depth (a) with time is often described by a relationship of the form:

$$a = \alpha t^{\beta} \qquad (3)$$

where α and β are system specific constants.

However, there are no data in the literature to establish the pit growth rate law for the blade steel, especially in environments and temperatures relevant to steam turbine operating conditions.

3.2 CORROSION FATIGUE

3.3.1 Effect of corrosion and pitting on the fatigue strength

The effect of pits as stress concentrators on a blade steel has been examined by Zhou and Turnbull[21]. They developed an electrochemical procedure to produce pits of a controlled depth and low density. The fatigue strength of the pre-pitted specimens was then measured in air. Tests were conducted at a fatigue frequency of 25 Hz with a stress ratio of 0.1 at ambient temperature. The fatigue strength was defined as the value of stress range below which the specimen did not fail above 1×10^7 cycles. The results showed that the fatigue strength for the specimens with 35 μm, 110 μm and 250 μm deep pits was 87%, 70% and 52%, respectively, of the fatigue strength of the "smooth" specimens (2400 grit finish). The dependence of the fatigue strength on pit depth was consistent with pits acting as effective short cracks of the same depth provided the El Haddad[26] short crack correction is used:

$$\Delta K = \alpha \Delta\sigma \sqrt{(a + a_0)} \qquad (4)$$

where ΔK is the range of the stress intensity factor, $\Delta\sigma$ is the stress range, α is a geometry factor, a is the pit depth and a_0 is a constant.

Lebedeva et al[27] also investigated the effect of pitting on fatigue resistance in blade steels (12%-13% Cr) using artificial pits. The aspect ratio of depth a to diameter d was 0.31 and the pit diameters are 0.4, 0.5 and 1.8 mm. Zhou and Turnbull[21] showed that the data by Lebedeva et al were also consistent with Equation (5), although with a different value of a_0.

The effect of corrosion/pitting on the fatigue strength of blade steels in NaCl, Na_2SO_4 and NaOH solutions has been well studied[6, 8, 17-20, 28]. Typical examples[18] of S-N curves for a blade steel in air, distilled water, and 3×10^{-4} % (3 ppm) to 3% NaCl solutions are shown in Figure 4 (f = 60 Hz and R = -1.0). The fatigue strength is reduced in 3% NaCl

solutions to about 25% of that in air at 10^7 cycles. They also reported that in 40% NaOH solution, the fatigue strength also decreased to about 25% of that in air at 10^8 cycles.

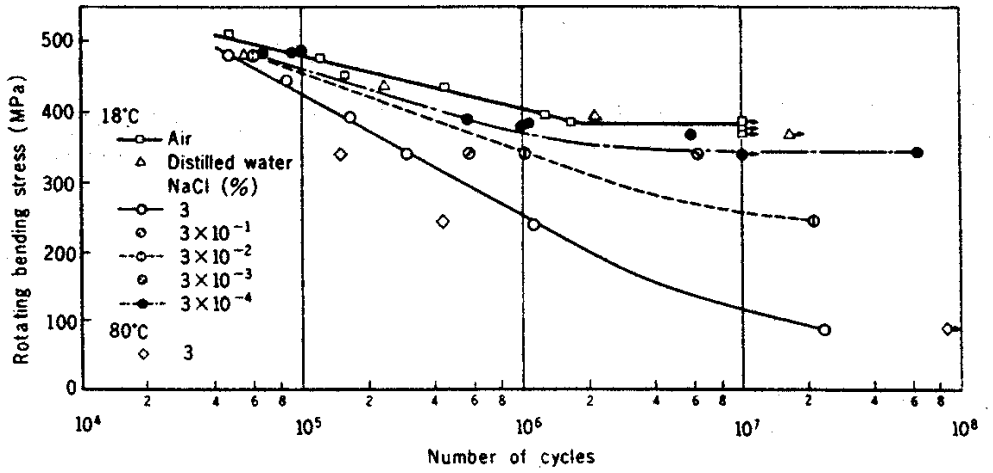

Figure 4. Effect of distilled water and NaCl concentration on the fatigue strength of a 12% Cr steel[18].

On the other hand, the reduction in the fatigue strength in 3×10^{-4} % (3 ppm) NaCl solution was modest, to about 85% of that in air. No reduction in fatigue strength was observed in distilled water. The authors did not report whether pits were observed in distilled water.

Shmitt-Thomas[25] also investigated the effect of corrosion on the fatigue strength of a number of blade steels in 0.01 M (0.059%) NaCl solution. The material compositions are listed in Table 3. Some results are shown in Figure 5. Again, there is a significant reduction in the fatigue strength in the NaCl solution compared with that in air and the extent of the reduction increases with temperature. It also demonstrated that the fatigue strength is significantly improved by the addition of 2.5% Mo (Figure 6).

Table 3. Chemical composition of tested steels[25].

Element	X4CrNiMo16-5-1	X20Cr13	X20CrMo13	X20CrMo13-2
C	0.028	0.19	0.20	0.26
Cr	15.1	13.3	13.5	12.6
Ni	5.1	-	-	-
Mo	0.92	0.03	1.04	2.41
Mn	0.83	0.53	0.67	0.60
Si	0.37	0.24	0.39	0.54
P	0.016	0.017	0.020	0.014
S	0.006	0.013	0.018	0.014
N	0.062	-	-	-

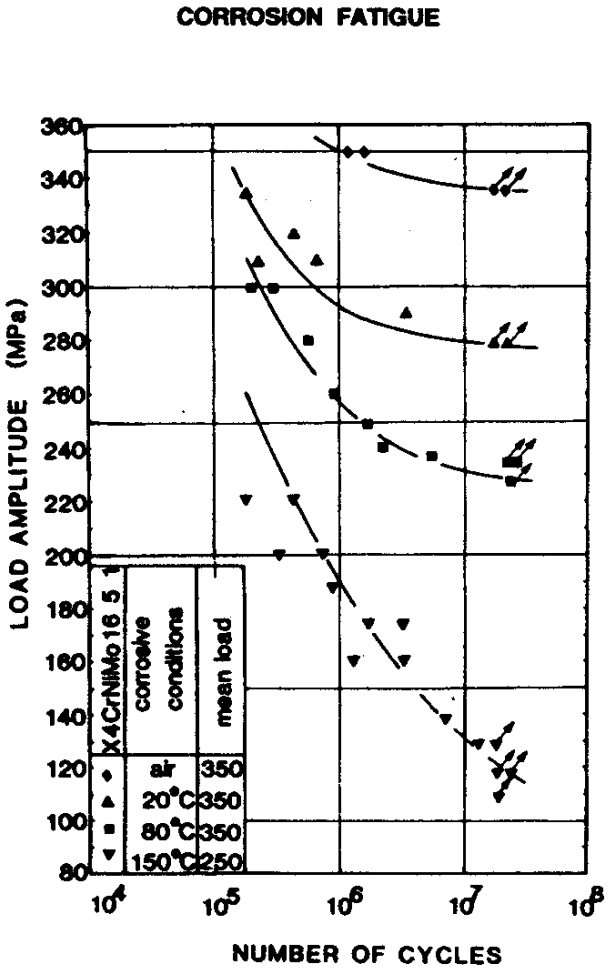

Figure 5. Corrosion fatigue behaviour of the soft precipitation hardening martensitic stainless steel X4CrNiMo16-5-1 at different temperatures in 0.01 M NaCl solution[25].

Lachmann[29] conducted low cycle fatigue tests under strain control with a triangular waveform on five turbine steels, three of which were blade steels. The tests were carried out with a strain rate of 1×10^{-3} s^{-1} and strain magnitude between 0.25% and 0.65% [of what?] in simulated boiler feed water (conductivity < 0.1 μS/cm at pH 7) at 20 °C and 90 °C (the calculated fatigue frequency was about 0.2 Hz). It was not specified whether the test water was circulated or refreshed and hence it was not clear whether the water conductivity was kept less than 0.1 μS/cm throughout the test. It was found that the simulated boiler feed water reduced fatigue life by a factor of 2 to 5 compared with the data in air, as exemplified in Figure 7. It was claimed that the temperature effect between 20 °C and 90 °C was negligible, in contrast to the findings in NaCl solution (Figures 4 and 5).

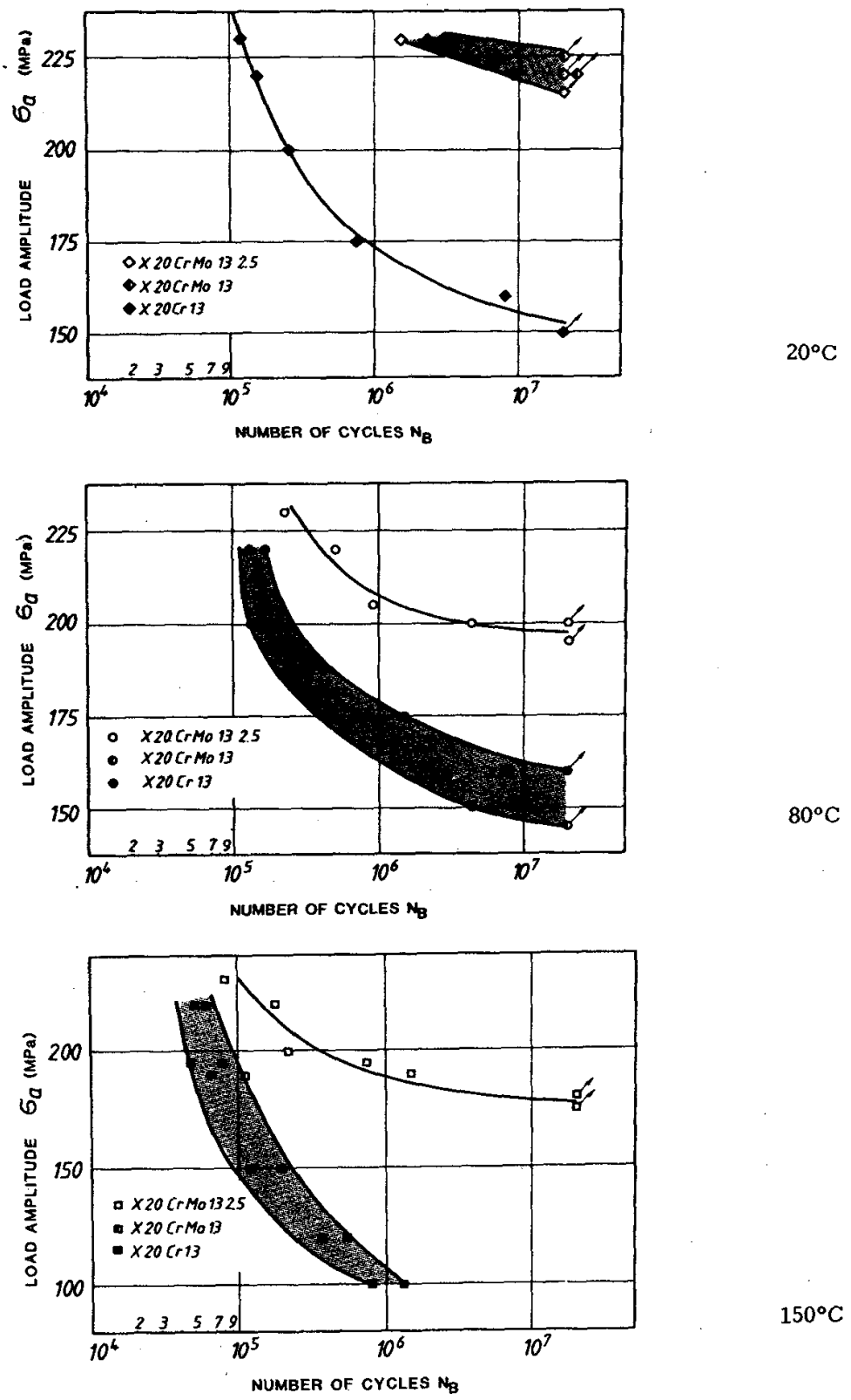

Figure 6. Corrosion fatigue behaviour of the martensitic stainless steel type X20Cr and its modifications with 1% and 2.5% Mo at different temperatures in 0.01 M NaCl solution[25].

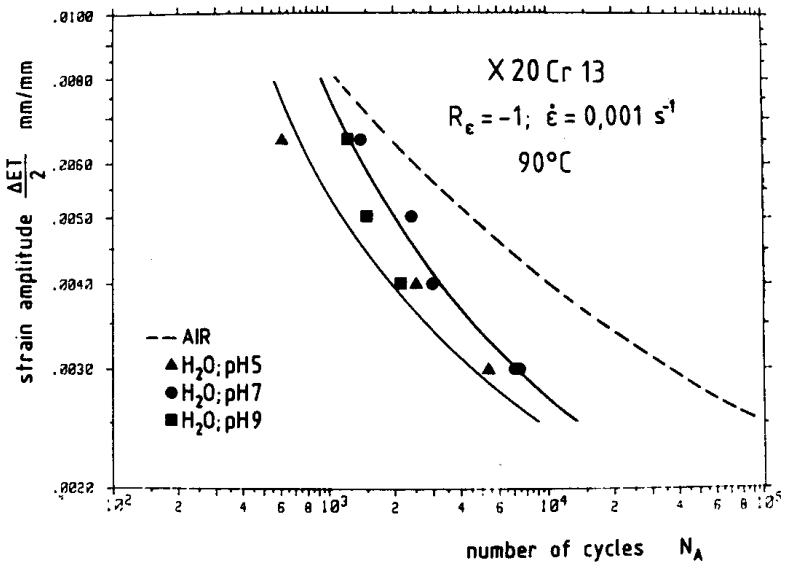

Figure 7. Total strain amplitude vs. number of cycles N_A forX20Cr13 in air and in feed water at various pH values[29].

Most of the fatigue tests of blade steels were conducted in aerated conditions, which may be too severe and unrealistic in the steam turbine applications[10]. The presence of oxygen increases the corrosion potential which in turn increases the risk of pitting or anodic dissolution if the steel is in the active state. Dissolved oxygen content has a significant effect on the fatigue strength of the blade steels[30], as shown in Figure 8. The fatigue strength in the deaerated solution at the same number of cycles is about three times higher than that in the aerated solution, but was lower than that in air. However, it should be noted that the fatigue tests were conducted at ambient temperature in air (like in many other studies) but at 80 ºC in solution. Therefore, the effect of temperature cannot be excluded from such a comparison.

More recently, Perkins and Bache[31] have studied corrosion fatigue of a 12% Cr low-pressure turbine steel in environments more relevant to the service conditions. Typical results are shown in Figures 9 and 10. It can be seen that the fatigue strength was slightly reduced even in the absence of oxygen and chloride, but the most detrimental effect was observed in 4 ppm oxygen + 1 ppm chloride solutions at 120 °C. They also reported that fatigue crack initiation occurred from corrosion pits in 4 ppm oxygen + 1 ppm chloride solutions at 120 °C, but these pits were only formed in the presence of cyclic stress.

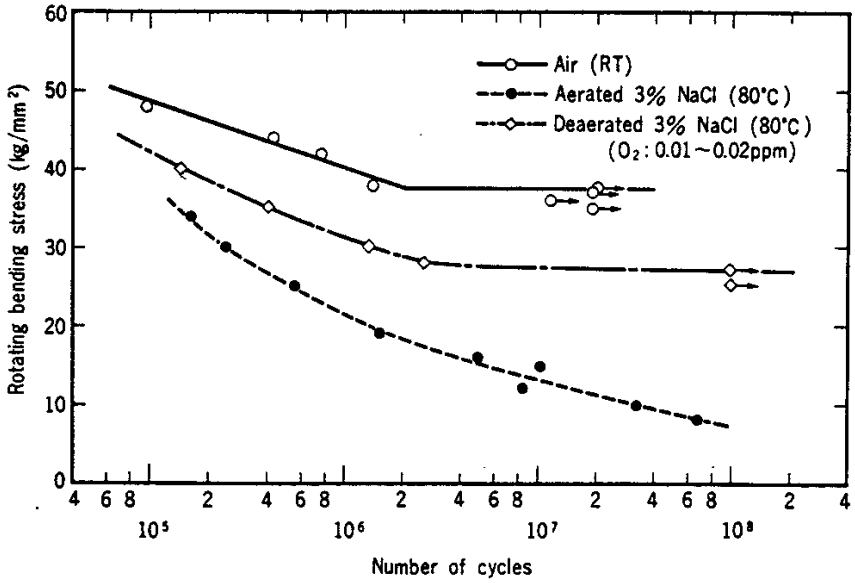

Figure 8. S-N curves of a turbine blade steel in air, aerated and deaerated 3% NaCl solution[30].

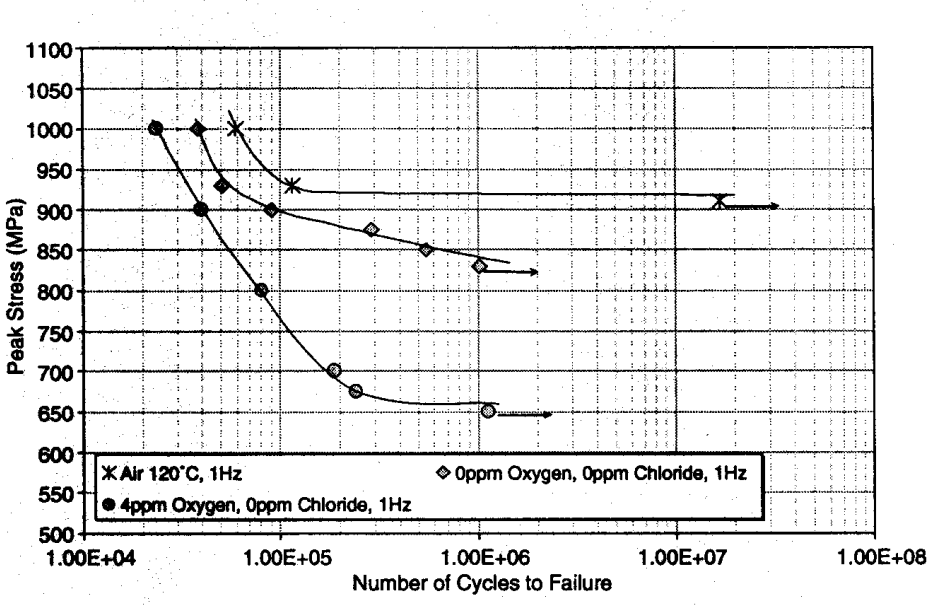

Figure 9. Effect of oxygen content on fatigue strength of FV566 in deionised water at 120 °C[31].

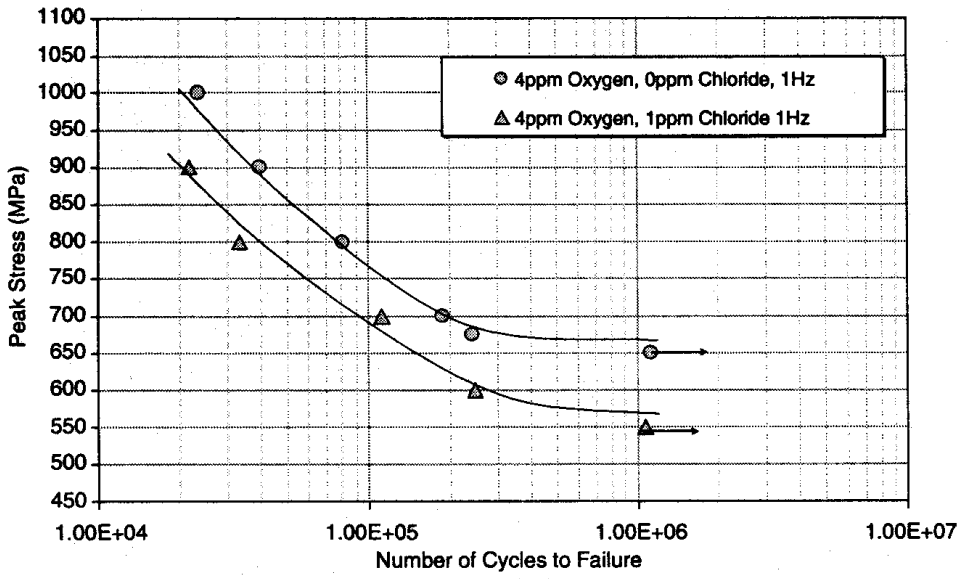

Figure 10. Effect of 1 ppm Cl^- addition on the fatigue strength in 4 ppm oxygen deionised water at 120 °C[31].

It has long been recognised that a fatigue limit does not exist under conditions where stable pits grow, as the threshold stress range for cracking decreases with the increase of the pit depth[32]. The fact that there is a plateau regime in the S-N curve of the blade steels, especially in water and relatively dilute chloride solutions or in the absence of oxygen (Figures 4, 5, 6, 8 –10), suggests that pits may only grow under certain dynamic strains or that pit growth rate is very slow after reaching certain depths.

All of the fatigue tests described above were conducted at high frequency and do not represent actual steam turbine service conditions. As stated earlier, the amplitude of high frequency cyclic loading associated with vibrations or steam bending is normally small and the low frequency (at most once per day for two shifting operating conditions) cyclic loading associated with start up/shut down is of more concern. It is well known that the environmental effect on the fatigue strength is time dependent, especially when pitting is a concern[32]. For instance, the growth rate of pits is low in the relatively benign environments associated with steam turbine operating conditions. In high frequency fatigue testing, the test duration (limited by the time to failure) depends on the level of stress range and can be as short as a few minutes at a high stress level. In this timescale, pits may not reach the critical size to promote crack initiation before fatigue failure occurs. Indeed, it has been found that at high stress (around the air fatigue limit), there is not enough time for pits to develop and hence the failure is mechanically dominated[32]. Therefore, lifetime prediction based on the S-N curves may seriously underestimate the impact of pitting, in the case where pitting is a precursor of crack initiation.

Another concern is that although the effect of environment and temperature on the fatigue strength is well studied, in most cases the comparison was made between the fatigue strength in air at ambient temperature and that in aqueous solutions at elevated temperatures. Therefore, the impact of environment on the fatigue strength could be overestimated as it is expected that the fatigue strength in air will decrease with increasing temperature.

3.3.2 Growth rate of fatigue cracks

The growth rate of fatigue cracks, da/dN, can generally be described by:

$$\frac{da}{dN} = C\Delta K^{m} \qquad (5)$$

where da/dN is the cyclic growth rate of fatigue cracks, ΔK is the range of the stress intensity factor, and C and m are constants.

The effect of environment on the fatigue crack growth rate of 13% Cr steel in 3% NaCl solution and in distilled water was investigated by Kawai and Kasai[28], as shown in Figure 11. It should be noted that it is unusual that a stress ratio of –1 was used for FM specimens because of crack closure. The crack growth rate at $K_{max} \geq 6$ MPa $m^{1/2}$ in 3% NaCl solution is nearly equal to the rate in air. However, the threshold stress intensity factor range, ΔK_{th}, and hence the maximum threshold stress intensity factor, $K_{max,}$ for the given stress ratio (R = -1) decreases to 2.5 MPa $m^{1/2}$ in the 3% NaCl solution, corresponding to only 42% of that in air. The reduction of the threshold stress intensity factor range for fatigue crack propagation was also observed by Ishii et al for a 13% Cr blade steel in 3% NaCl solution[33]. This is not surprising, as the environment is not expected to have an effect on the fatigue crack growth rate at the high cyclic frequency (35 Hz), as the growth rate is dominated by the mechanical damage processes. However, the threshold stress intensity factor range for fatigue crack propagation would decrease in aggressive environments, because corrosion may dissolve the microstructural barrier (e.g. grain boundary) to crack propagation[24].

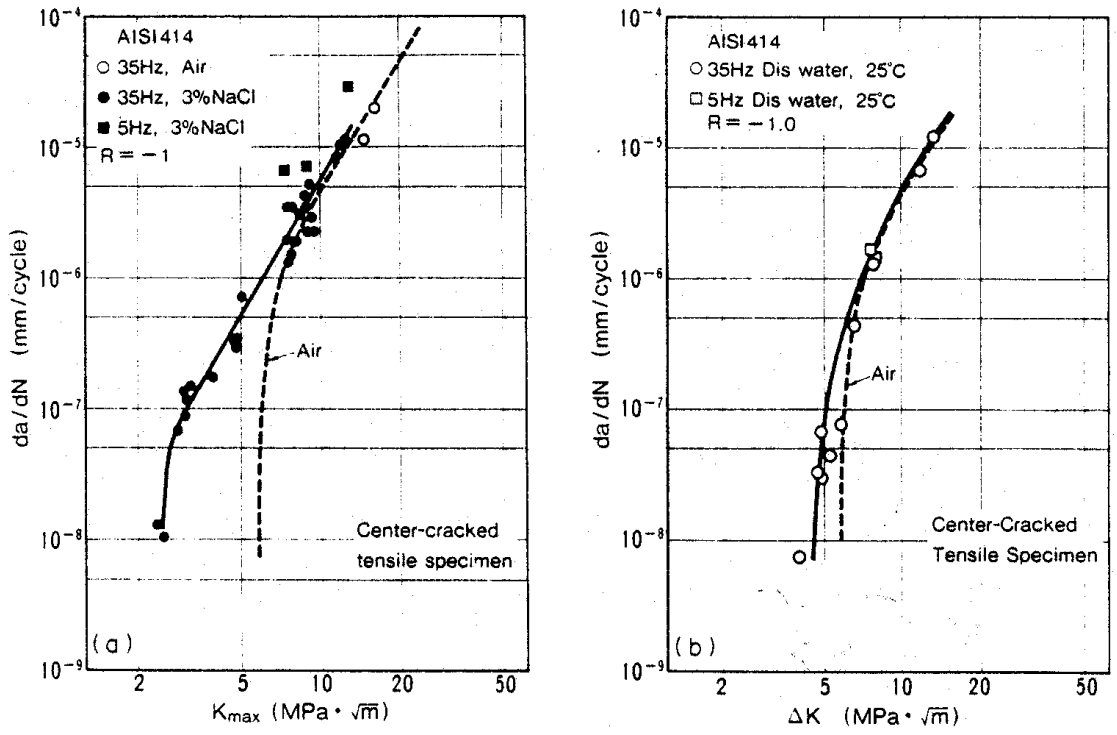

Figure 11. Environment effect on the growth rate and the threshold stress intensity factor range of fatigue cracks in a 13% Cr stee[28].

Gabetta and Torri[19] reported that the crack growth rate was much higher in 22% NaCl solution at 80 ºC than that in air, as shown in Figure 12 (f = 50 Hz, R = -1). However, as the crack growth rate in air was measured at ambient temperature, the difference in the crack growth rates is possibly related to the difference in test temperatures instead of the effect of environment.

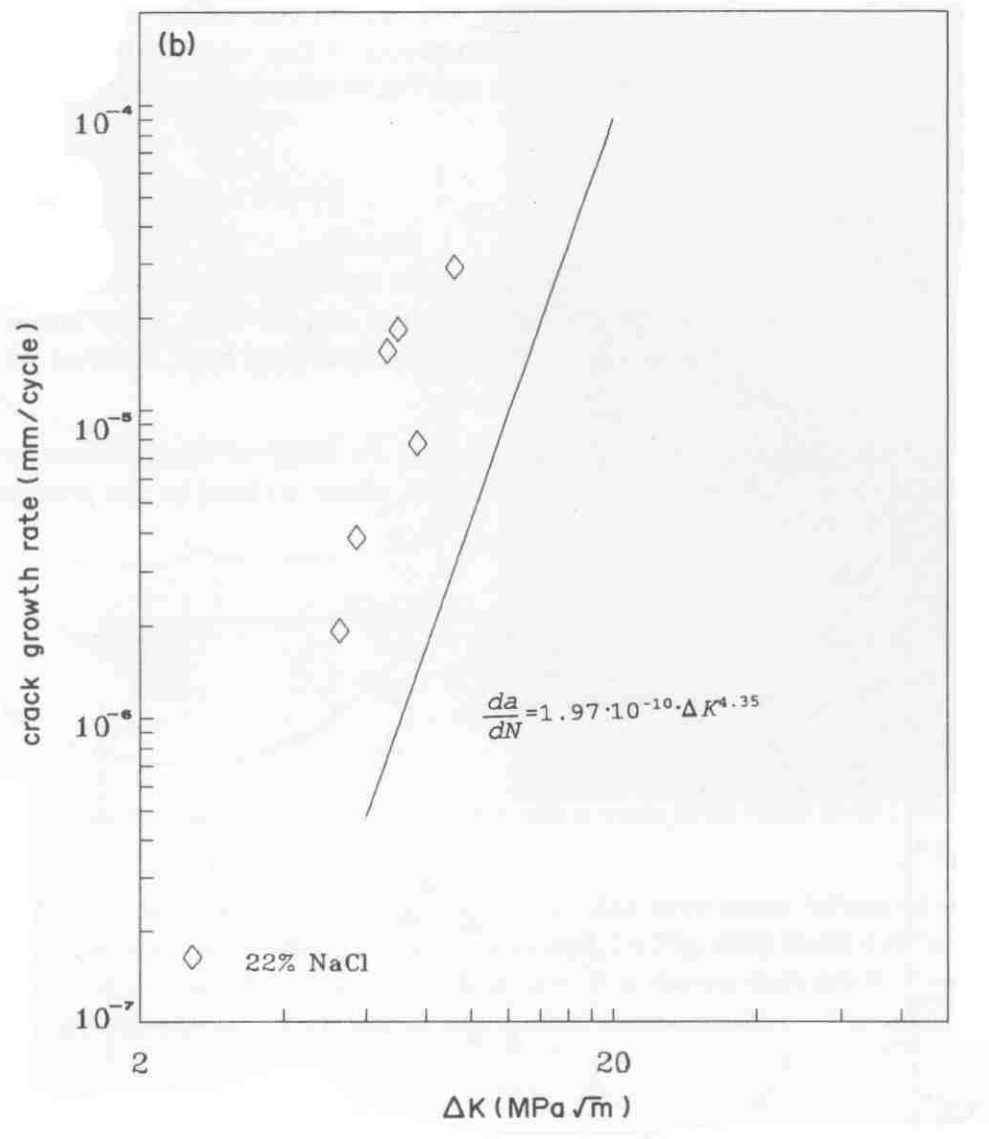

Figure 12. Fatigue crack growth rate of a 12% Cr blade steel in air at 22 °C and in 22% NaCl solution at 80 °C[19].

The growth rate of fatigue cracks of a 12% Cr blade steel in 3.5 % NaCl, 12.7% Na_2SO_4 and distilled water at 25 ºC, 60 ºC, 90 ºC and 150 ºC was measured by Cho et al[34], as shown in Figure 13 (R = 0, f = 0.5 Hz). At the same temperature, the growth rate was similar in the different environments. However, there was a significant effect of temperature on the crack growth rate in all environments.

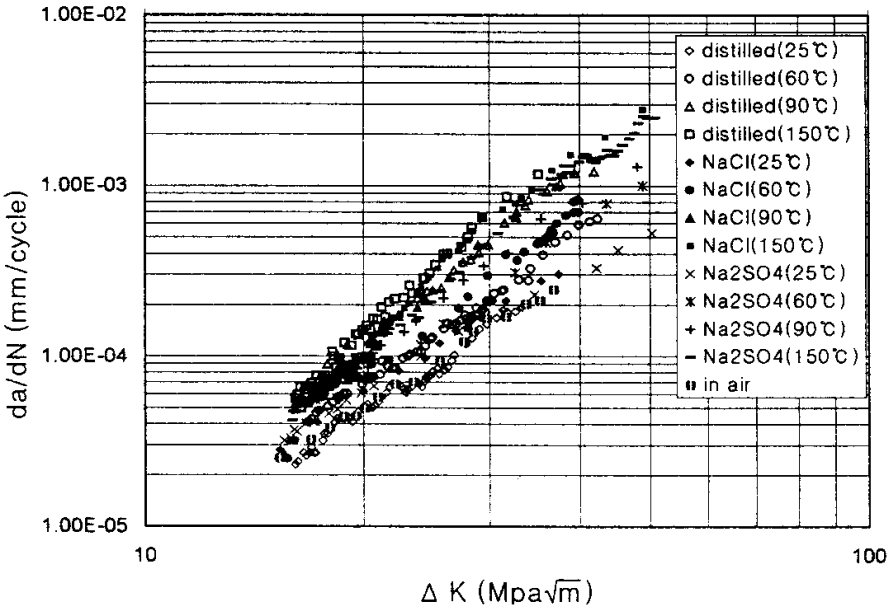

Figure 13. The cyclic growth rate of fatigue cracks in 12% Cr steel as a function of ΔK in various environments[34].

Again, it should be noted that the effect of environment on the crack growth rate of blade steels has been assessed mainly under high frequency cyclic loading. It is well known that crack growth under high frequency fatigue is mechanical damage dominated and there is not sufficient time for the reaction between the new surface at the crack tip and the solution. Therefore, the impact of environment on crack growth rate cannot be fully assessed under high frequency cyclic loading conditions.

The crack growth rate of a 12% Cr blade steel (Type FV566) was determined at NPL under trapezoidal loading (load up: 20 min, load hold: 100 min, load down: 20 min and load off: 20 min) to simulate approximately the two shifting operating conditions. The environment was 300 ppb Cl^- + 300 ppb SO_4^{2-} solution at 90 °C to simulate the water chemistry of the condensates on load but the solution was aerated to take into account the aeration during off load and the possible prolonged effect of the slow decay in the corrosion potential of the steel after the transition from aerated to deaerated conditions[23]. The results are shown in Figure 14, together with the growth rate of fatigue cracks in air at the same temperature. Comparison of the crack growth rate also shows that there is a marked effect of the environment, as the crack growth rate in the solution is about 10 times higher than that in air.

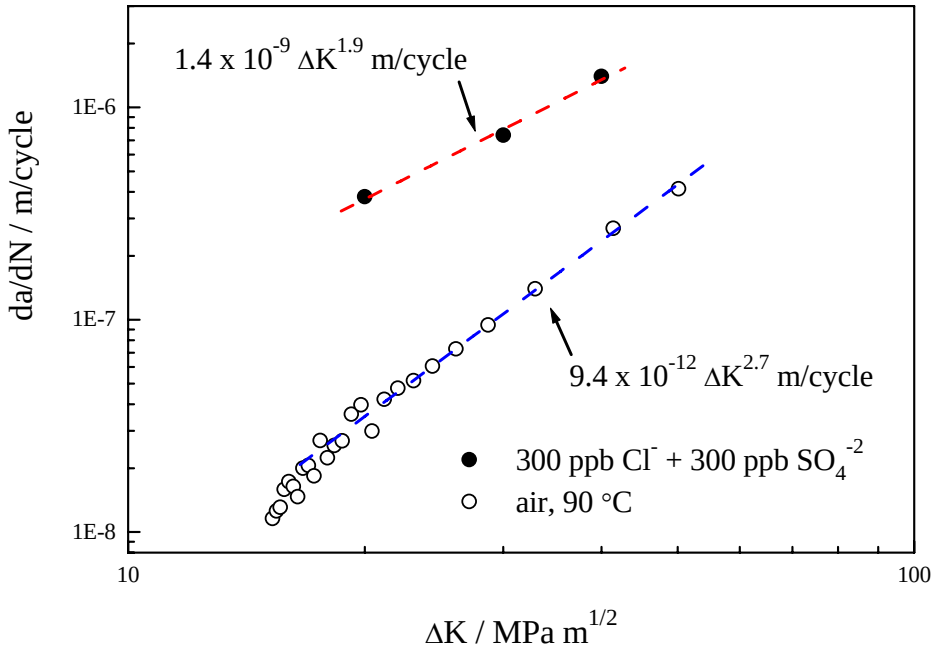

Figure 14. Comparison of crack growth rates for the blade steel in aerated 300 ppb Cl^- + 300 ppb SO_4^{2-} solution at 90 °C with test data obtained in air also at 90 °C[23].

3.3 STRESS CORROSION CRACKING

Stress corrosion cracking studies have mainly been carried out in concentrated NaCl and NaOH solutions and, unlike for the disc steels, there have been few long-term stress corrosion tests conducted in water or dilute solutions representing more realistically the water chemistry of the condensates formed on the blade surface.

Figure 15 shows the growth rate of stress corrosion cracks in a 12% Cr blade steel under static stress in aerated 22% NaCl solution at 105 °C and in aerated deionised water at 23 °C[35]. The threshold stress intensity factors for SCC, K_{ISCC}, for the blade steels studied are listed in Table 4. It can be seen that the environment (and temperature) have a significant effect on K_{ISCC}.

Table 4 K_{ISCC} for blade alloys[35].

Alloy	Environment	K_{ISCC} / MPa $m^{1/2}$
X20CrMoV12-1	H_2O, 23 °C	> 100
	22% NaCl, 105 °C	35
X5CrNiMoCuNb15-4	22% NaCl, 105 °C	26
X4CrMnNiMoN26-6-4	4M NaCl, pH 2-16, 80°C	>60
Ti-6Al-4V	22% NaCl, 23 °C	32

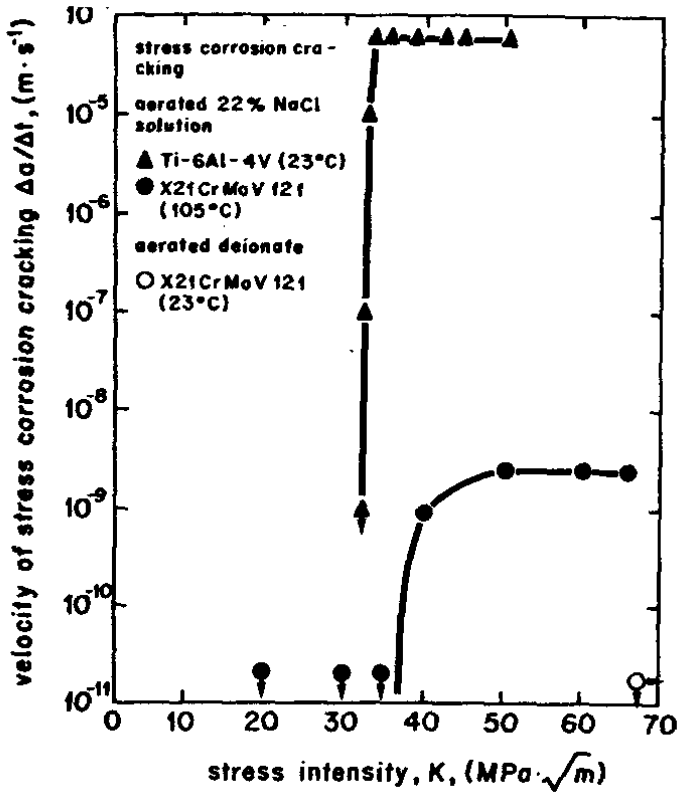

Figure 15. Stress corrosion resistance of blade steels[35].

Sparkes studied the stress corrosion crack growth rate of two blade steels, FV566 steel[11] and FV520B[36] in deaerated deionised water, oxygenated deionised water (35 ppm O_2) and refluxing 30% NaOH at 120 °C. The FV566 steel had 11% - 12 % Cr and the proof stress, $\sigma_{0.2}$, was 900 MPa when tempered at 630/650 °C and about 1000 MPa when tempered at 600 °C), while the FV520B steel had 14.4% Cr and $\sigma_{0.2}$ was 1020 MPa for standard and 1290 MPa for fully hard. The tests were conducted using wedge opening load (WOL) specimens and the average crack growth rate was calculated after exposure to the solutions for various durations. The results are shown in Figures 16 –19.

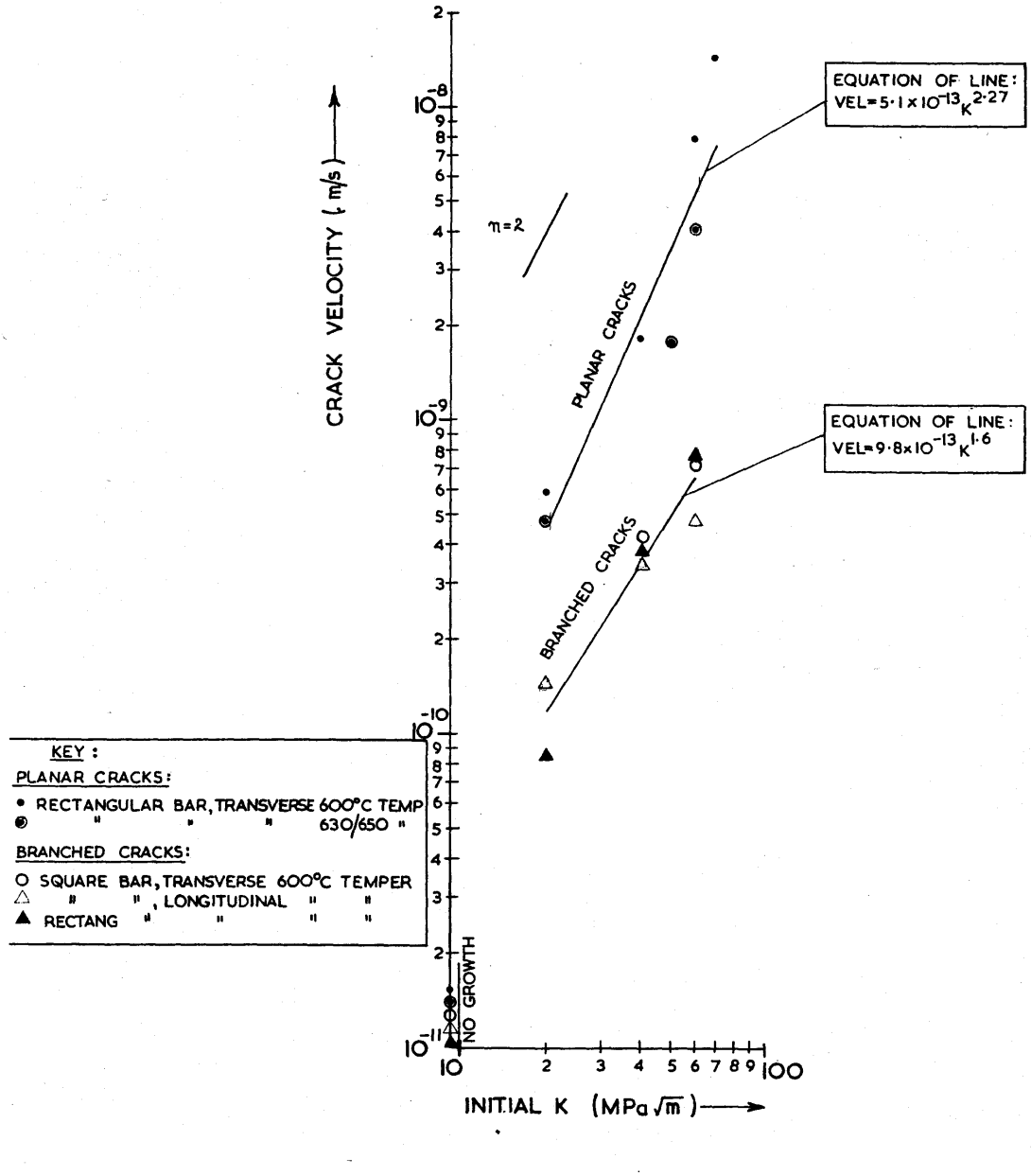

Figure 16. Effect of stress intensity factor on the stress corrosion crack growth rate of FV566 exposed to refluxing 30 % NaOH solution at 120 °C[11].

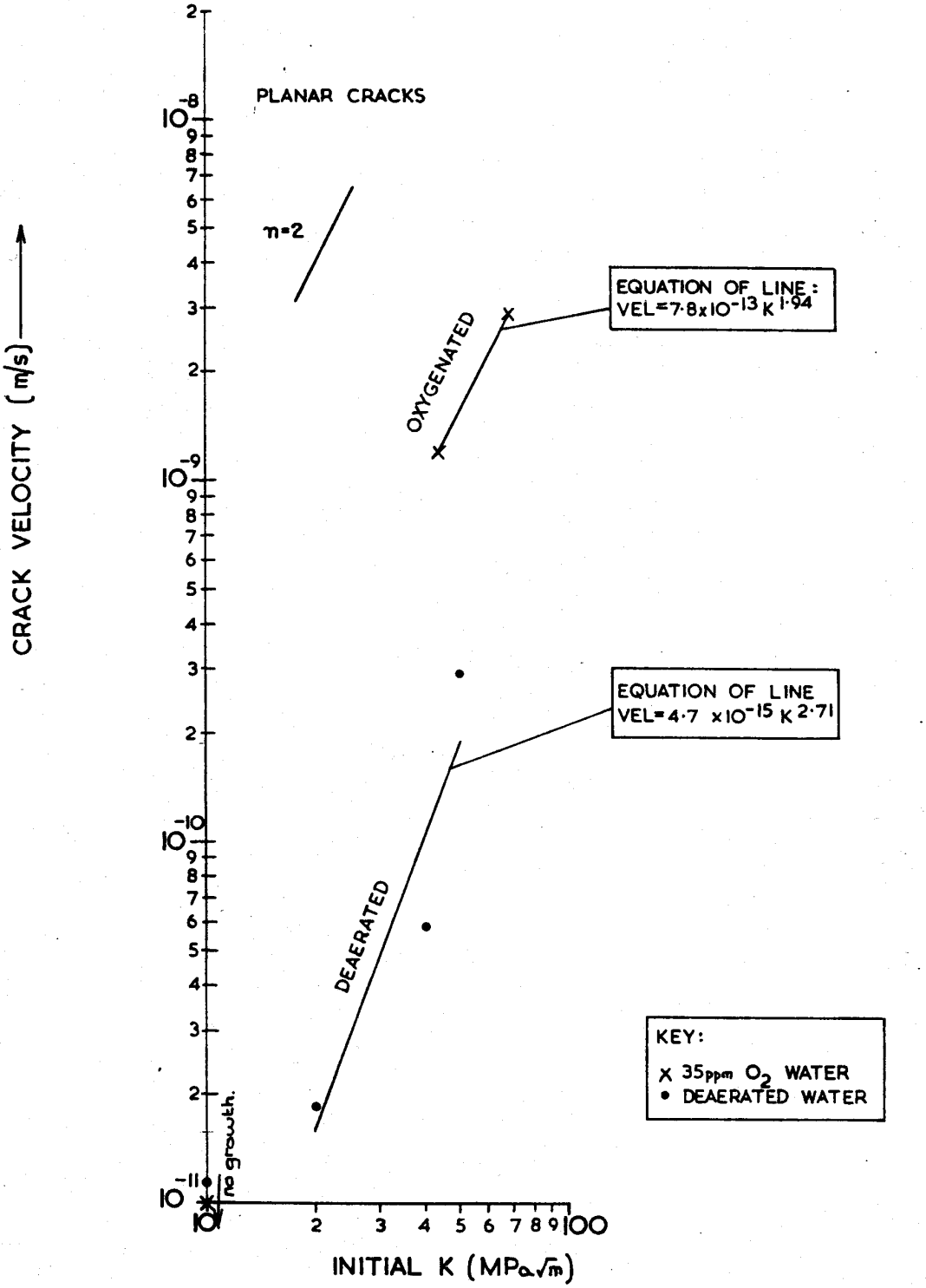

Figure 17. Effect of stress intensity factor on the stress corrosion crack growth rate of FV566 exposed to deaerated and oxygenated water at 120 °C[11].

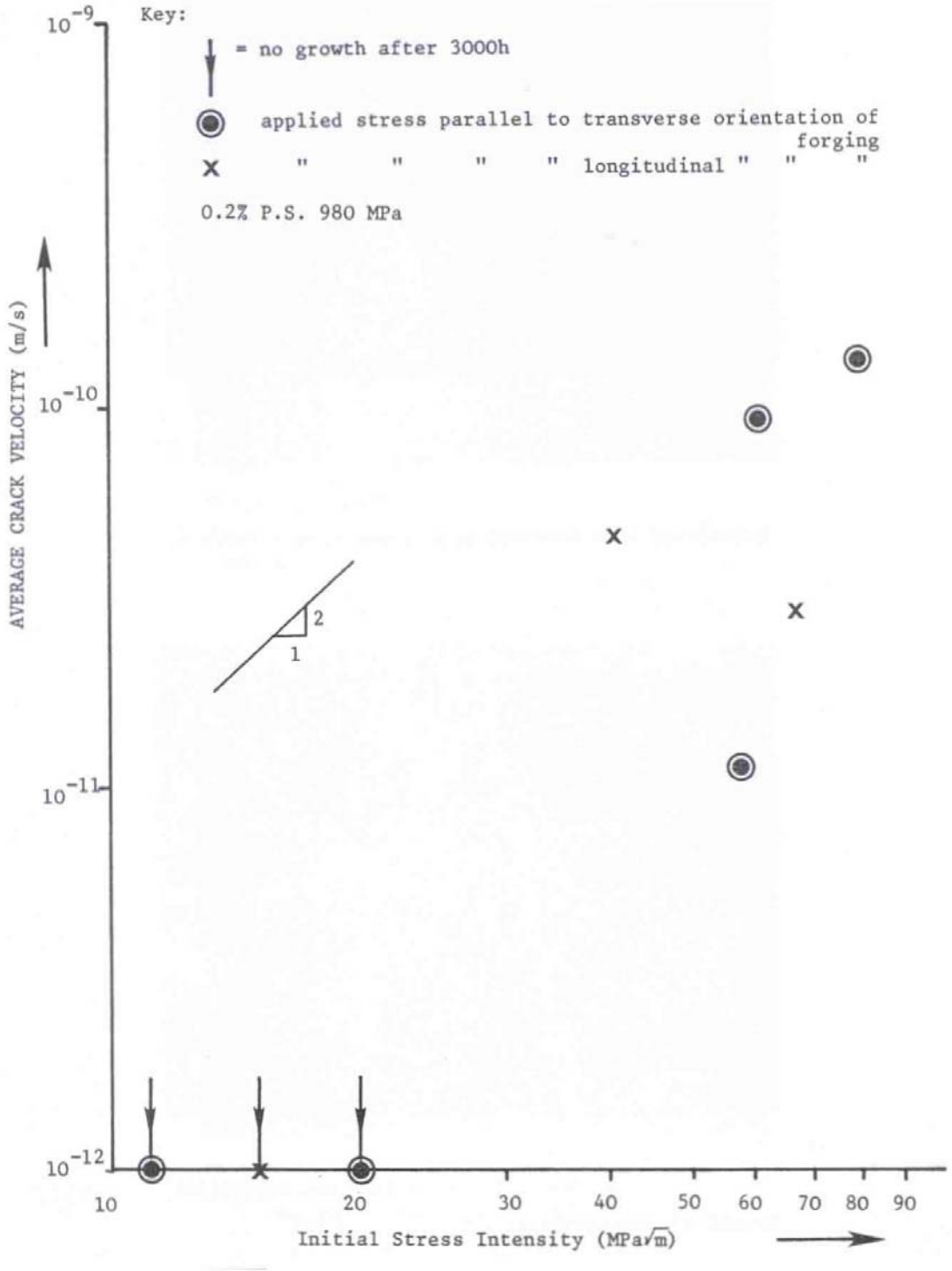

Figure 18. Effect of stress intensity factor on the stress corrosion crack growth rate of standard condition FV520B exposed to refluxing 30 % NaOH solution at 120 °C[36].

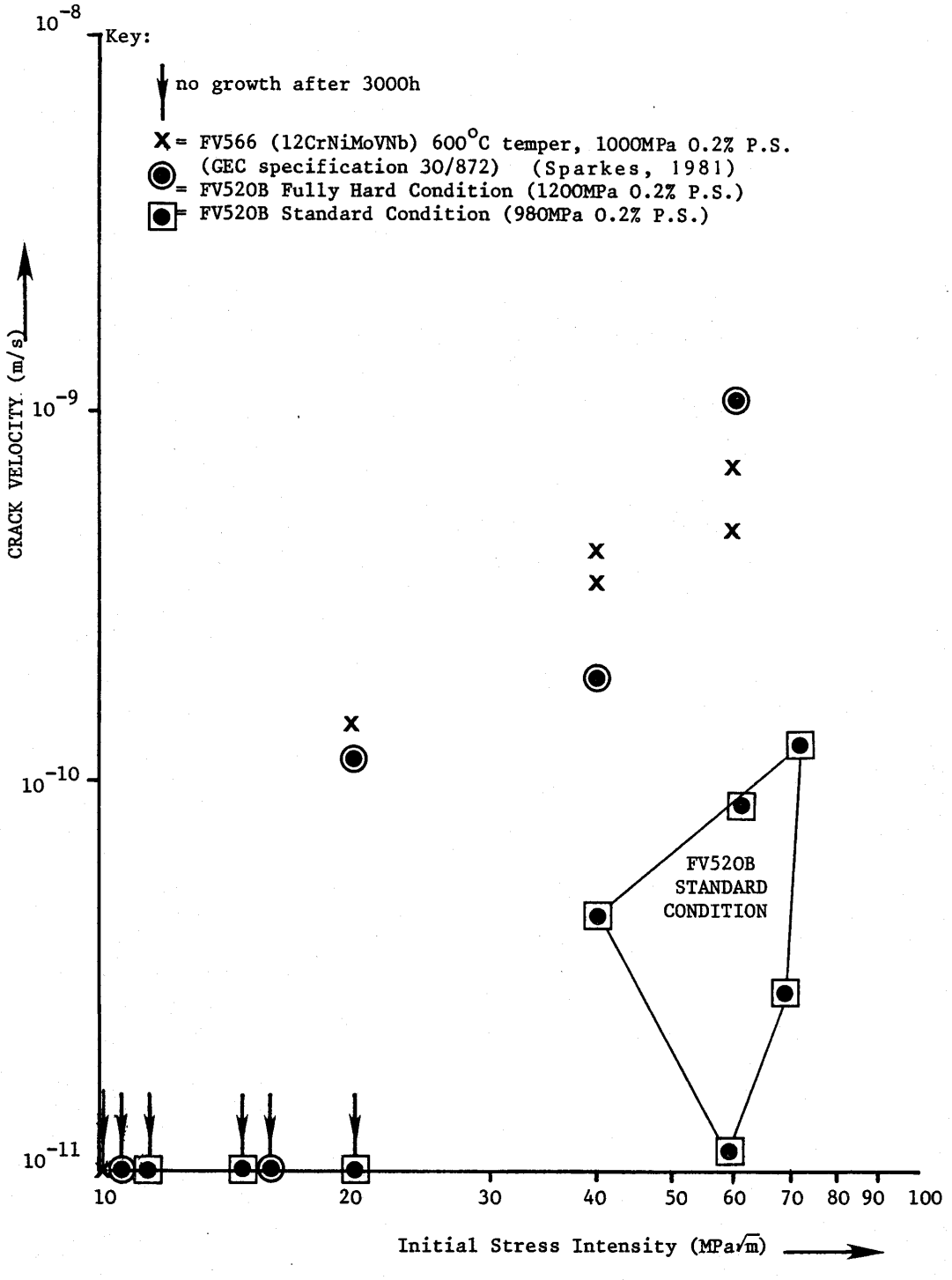

Figure 19. Comparison of stress corrosion cracking susceptibility of FV520B and FV566 turbine blade steels in 30% NaOH solution at 120 °C[36] (note: 30/872 in the figure should be 30/372).

The K_{ISCC} for FV 566 was less than 20 MPa $m^{1/2}$, even in the deaerated water at 120 °C. For FV520B, K_{ISCC} was also less than 20 MPa $m^{1/2}$ for the fully hard condition and in the range of 20 MPa $m^{1/2}$ to 40 MPa $m^{1/2}$ for the standard condition in refluxing 30% NaOH solution at 120 °C. No crack propagation was observed in fully hard FV520B tested for 4466 h at 72 MPa $m^{1/2}$ in aerated water or in standard FV520B tested for 5256

h at 61 MPa $m^{1/2}$ in deaerated water at 120 °C. However, Sparkes suggested that the K_{ISCC} would be expected to be the same as that obtained in 30% NaOH solution[36] and that the fact that no cracking was observed at stress intensity factors well above these values was probably because the initiation time for cracking in water exceeded 5000 h. The author quoted other work[37] that reported crack initiation periods for precracked WOL specimens exposed to water/steam of up to 8000 h.

The threshold stress intensity for cracking of FV566 and FV 520B was much lower than that of X21CrMOV12-1 in 22% NaCl at 105 °C obtained by Attrens et al, although the Cr (12% mass) content in X21CrMOV12-1 is similar to that of FV566 and lower than that of FV 520B. However, it is difficult to make a full comparison as the concentration of minor elements in X21CrMOV12-1 and the mechanical properties were not given. It should also be noted that X21CrMOV12-1 is typically tempered (at Alstom) at ~700 °C and gives a lower yield stress than FV566 and FV520[4].

Two interesting findings should be noted in the above work. One is that crack growth is approximately proportional to the square of the stress intensity factor over the range studied and there is no regime independent of the stress intensity factor, in contrast to other work. The other is that the crack growth rate seems surprisingly high, even in deaerated water (of the order of 10^{-10} m/s).

Zhou and Turnbull also measured the crack growth rate of a 12% Cr blade steel in aerated 300 ppb Cl^- + 300 ppb SO_4^{2-} solution at 90 °C at static stress using FM specimens and pulsed DCPD crack monitoring technique. The growth rate at a stress intensity factor of about 40 MPa $m^{1/2}$ was very low, about 4.6 x 10^{-12} m/s (0.14 mm/y).

The reason for the high growth rate obtained by Sparkes is not obvious as the water chemistry appears to be tightly controlled. One possibility is the high S (0.012% - 0.035% mass) and P (0.015% -0.022%) contents in the steel used by Sparkes[11] (the steel used by Zhou and Turnbull had < 0.003% mass S and <0.009% mass P).

3.4 CRACK MORPHOLOGY

As discussed earlier, for smooth specimens the corrosion fatigue cracks are often initiated from corrosion pits, especially in the presence of chloride and oxygen. A typical example[18] in which the crack was developed from a pit of about 20 μm in surface diameter is shown in Figure 20. Pitting was also reported[31] to be responsible for crack initiation in 4 ppm oxygen + 1 ppm Cl^- solution at 120 °C, as shown in Figure 21.

The fatigue and corrosion fatigue cracks were reported to be mixed intergranular / transgranular mode. The fraction of intergranular fracture was small near the crack initiation region[18]. It increased and then decreased with the maximum stress intensity factor, K_{max}, as shown in Figure 22. It can also be seen that the area fraction of intergranular fracture increased with the presence of NaCl, but there was little change in the value of K_{max} at which the area fraction of intergranular peaked. A similar transition of crack mode from transgranular to intergranular was also observed in both aerated and deaerated water at 120 °C[31]. However, the change of fracture mode does not necessarily indicate the transition of the fracture mechanism from anodic dissolution to hydrogen embrittlement, as claimed by the authors, since the transition of fracture mode may occur simply due to the change in the value of ΔK.

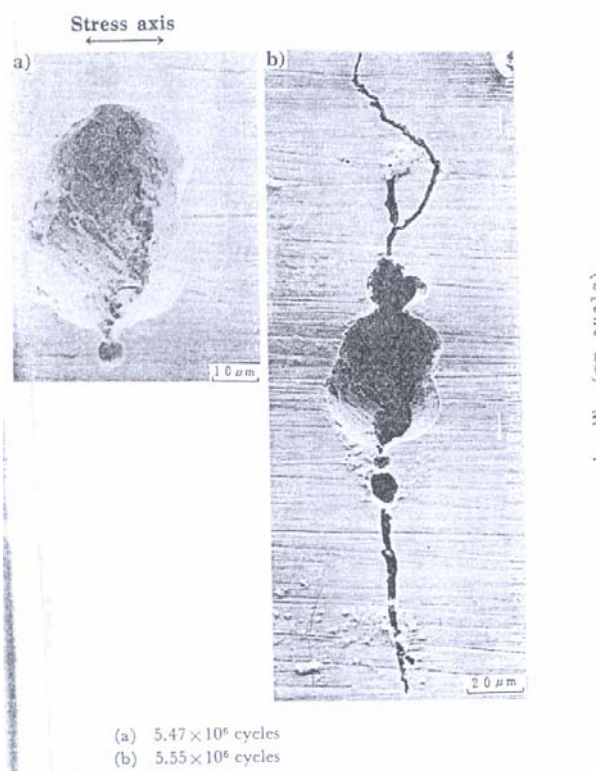

Figure 20. Crack initiation and propagation from corrosion pit, plane bending stress: 228 MPa, 3% NaCl solution at 45 °C[18].

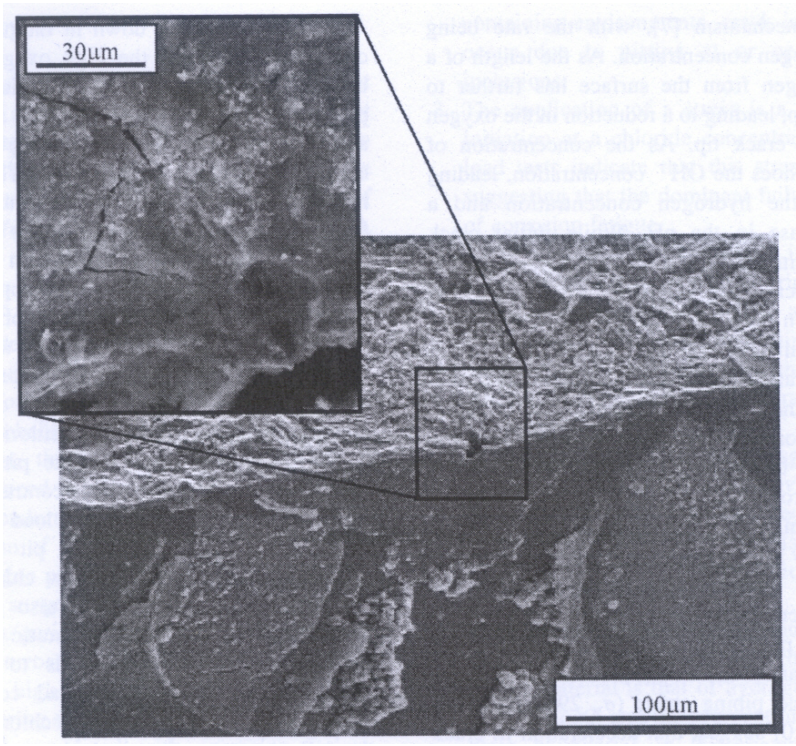

Figure 21. Fatigue initiation as a result of pitting on specimen surface tested in 4 ppm oxygen + 1 ppm Cl^- solution at 120 °C[31].

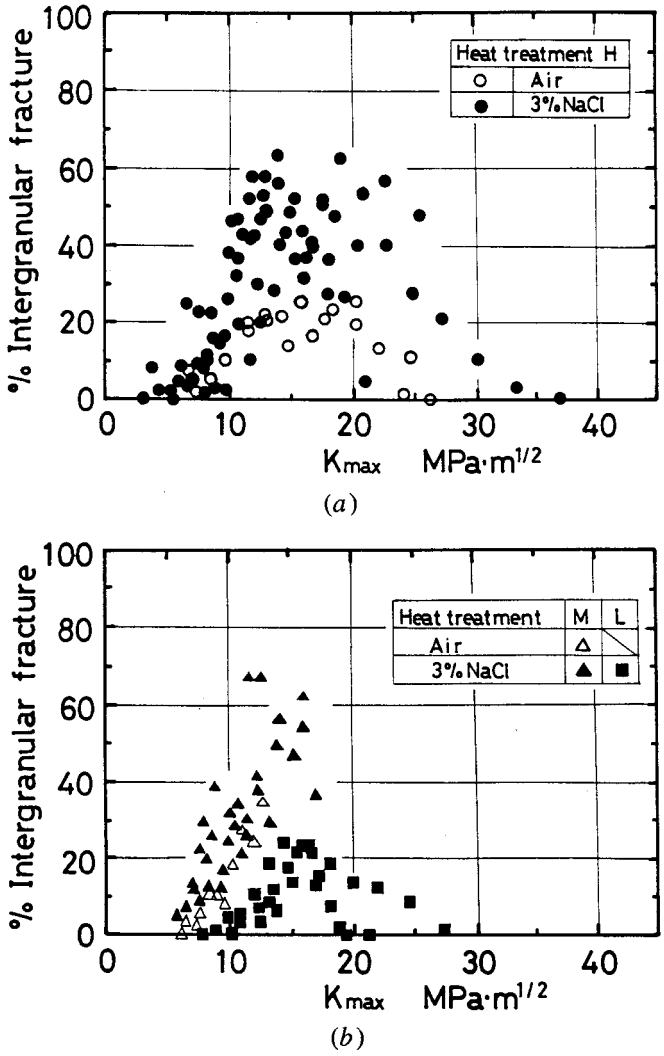

Figure 22. Area percentage of intergranular fracture of a 13% Cr blade steel as a function of the maximum stress intensity factor, K_{max}[18].

The stress corrosion crack morphology of FV566 in 30% NaOH solution was also found to depend on the stress intensity factor. When planar crack propagation occurred the crack mode was exclusively transgranular at K values of 50 MPa $m^{1/2}$ or above and mixed intergranular/transgranular at K values of 40 MPa $m^{1/2}$ or less (Figure 23). When crack macro-branching occurred the substantial reduction in the K value resulted in mixed mode cracking at all initial K values (Figure 24).

It was also reported by Sparkes that the stress corrosion crack morphology in deaerated and aerated water was the same as observed in 30% NaOH, as shown in Figure 25.

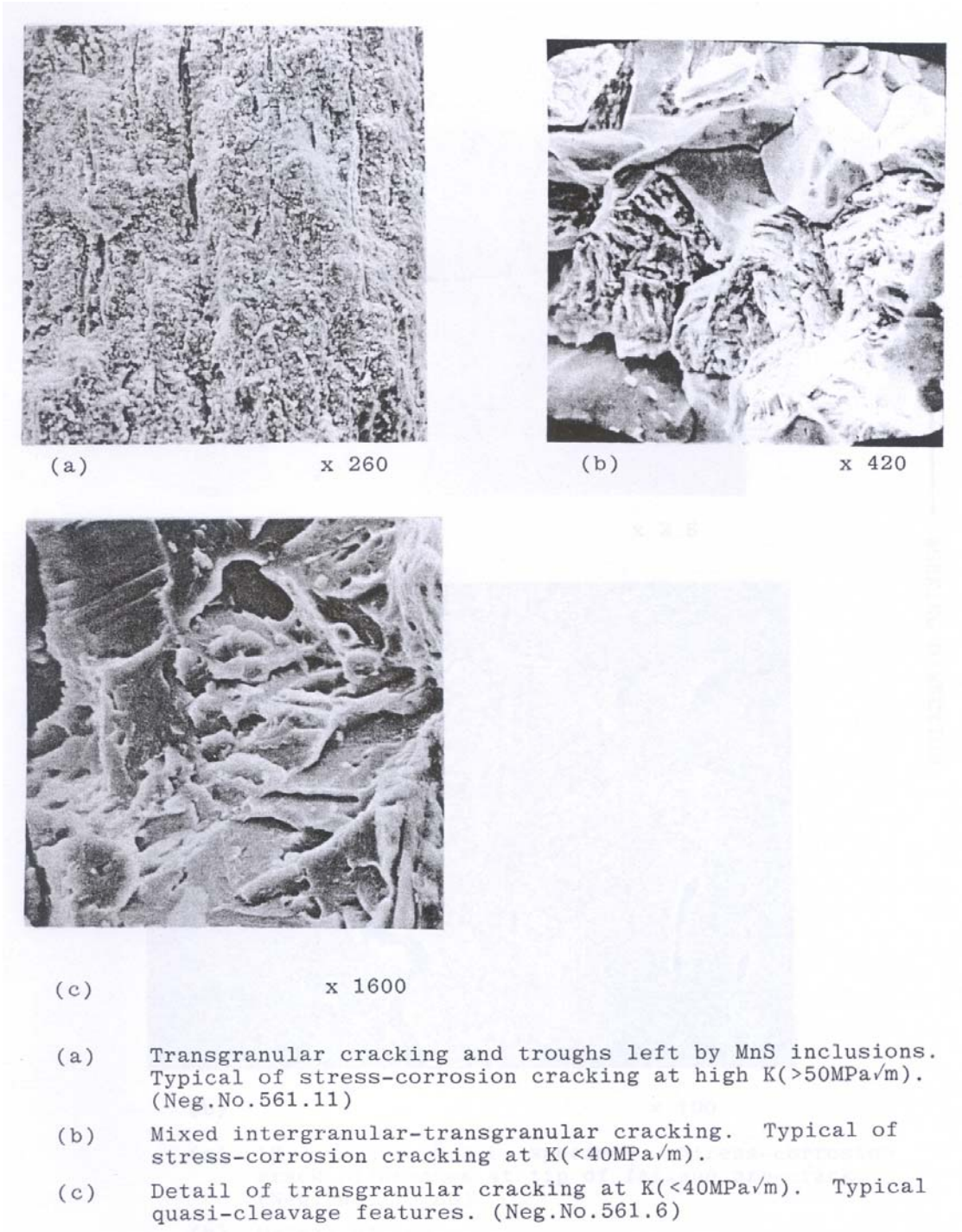

Figure 23. Stress corrosion fracture surfaces for FV 566 in 30% NaOH at 120 °C[11].

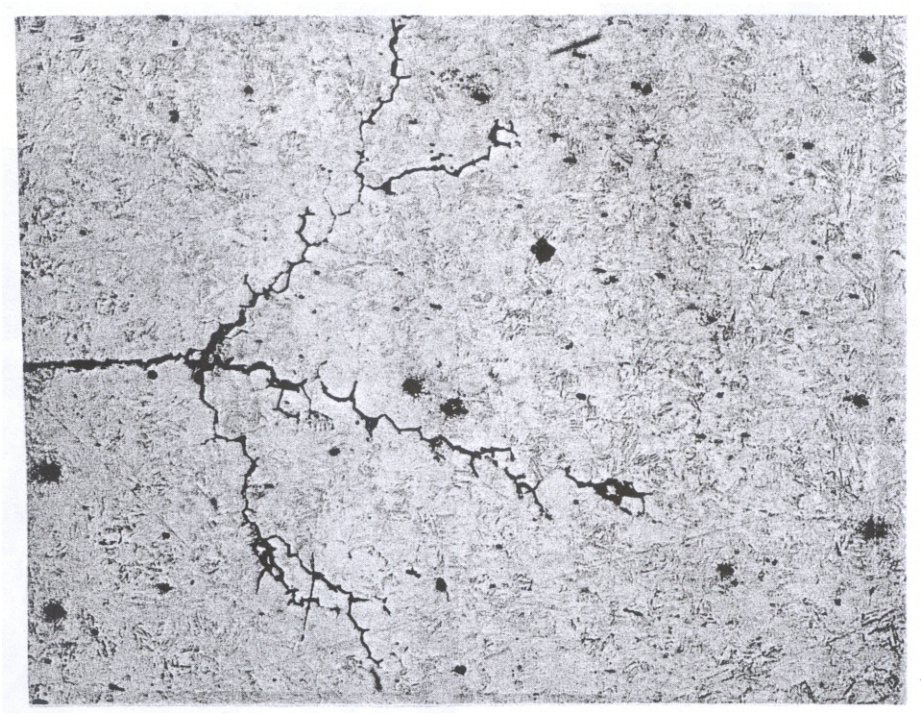

Figure 24. Stress corrosion crack propagation[11] in FV566 exposed to 30% NaOH for 426 h at an initial K value of 60 MPa $m^{1/2}$.

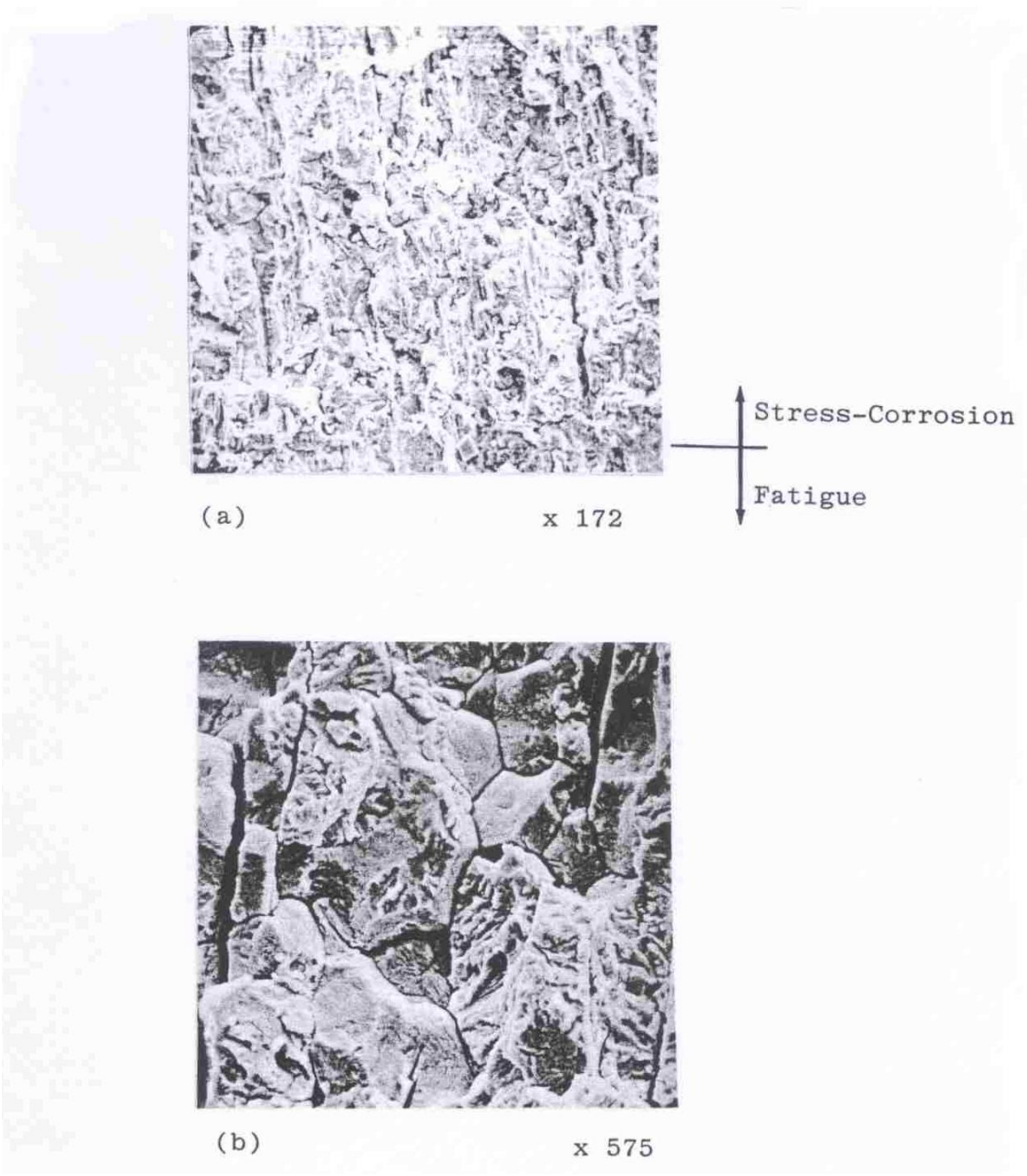

Figure 25. Stress corrosion fracture surfaces for FV 566 in water at 120 °C[11], a) transgranular cracking (K > 50 MPa $m^{1/2}$ and b) mixed intergranular – transgranular cracking (K < 40 MPa $m^{1/2}$).

4. CONCLUSIONS

- The susceptibility of blade steels to pitting was dependent on the material composition (Cr, Mo and W), chloride concentration and temperature. For a 12% Cr blade steel (FV566) in the absence of dynamic stain, the critical chloride concentration for pitting was greater than 500 ppm in aerated solution (1.8 ppm O_2) at 90 °C. This chloride concentration is much higher than would be expected in a steam turbine condensate under normal operating conditions.

- Pitting of blade steels occurred more rapidly under cyclic stress. However, it was reported that the pits in 3×10^{-4} % to 3% NaCl at ambient temperature were all shallow (less than 20 μm deep) and independent of test time, suggesting that these were non-propagating pits, probably assisted by fatigue but limited due to dissolution of near-surface MnS inclusions.

- There was a significant effect of environment on the fatigue strength of blade steel in concentrated NaCl and NaOH solutions, with no evidence of a fatigue limit. In aerated water, the findings were inconsistent in different laboratories, ranging from no effect to a reduction in fatigue strength to 75% of that in air. One result suggested that the fatigue strength in deaerated water was about 90% of that in air.

- There was no significant effect of environment on the growth rate of fatigue cracks in the moderate to high ΔK regime, as the tests in the literature were usually conducted at relatively high frequency. However, a reduction of the threshold stress intensity factor range for cracking was observed in 3% NaCl solution, probably because corrosion dissolves the microstructural barriers to crack propagation.

- Stress corrosion cracking of the blade steel has not been well studied. Limited results showed that both the threshold stress intensity for cracking and the crack growth rate were strongly dependent on the chemical composition of the steels with high impurity levels a likely factor in some results.

- The fatigue cracks were mixed intergranular and transgranular mode. The fraction of intergranular fracture increased and then decreased with increasing maximum stress intensity factor. For stress corrosion cracks, the mode changed from intergranular to transgranular with increasing stress intensity factor, in 30% NaOH solution, deaerated water and oxygenated water at 120 °C.

5. RECOMENDATIONS

- Further studies are required to establish the critical water chemistry (chloride and sulphate) for pitting of the blade steel at the temperatures of interest. Also, it is desirable to generate data on the dependence of pit growth rate on the pit depth in environments that represent the steam turbine service conditions more realistically.

- The existing data on the growth rate of fatigue cracks have mainly been generated under high frequency fatigue loading, which is not particularly relevant to the steam turbine operating conditions. It is important to generate data on the crack growth rate at a frequency similar to that in the start up/shut down cycles associated with two shifting practice and in environments more closely representative of the water chemistry of the condensates on the blade surface.

- SCC data, both threshold stress intensity factor for cracking and the crack growth rate, are scarce and this requires further study, especially in environments relevant to the low pressure turbine applications.

6. ACKNOWLEDGEMENTS

This work was conducted as part of the Materials Performance programme, a joint venture between the United Kingdom Department of Trade and Industry and an Industrial Group comprising Douglas Gass (Siemens), Sarah Harris (BNFL Magnox), Stuart Holdsworth (Alstom), Paul McIntyre (IOMMM), Paul Mulvihill (Powergen), Terry Parsons (BNFL Magnox), Neville Shaw (RwenPower) and Mike Tookey (British Energy). The author is grateful to B.W. Roberts (Alstom) for helpful comments.

7. REFERENCES

1. A. Turnbull and S. Zhou, Corrosion Engineering, Science and Technology, Vol. **38**, No.3, p.177, 2003.
2. J. R. Missimer, The Problems and the Solutions, Salt Lake City, Utah, USA, 2-6 December, 1985, pp. 81-86.
3. Corrosion Fatigue of Steam Turbine Blade Materials, Workshop Proceedings, Ed. R. I. Jaffee, Palo Alto, California, USA, 21-24 September 1981.
4. B. W. Roberts, Alstom, Private communication, 2006.
5. M.O. Speidel and B. Scarlin, 'Stress corrosion cracking and corrosion fatigue of steam-turbine rotor and blade materials', Proc. High Temperature Materials for Power Engineering, Liege, Belgium, 24-27 Sept, 1990, pp 343-368.
6. A. V. Ryabchenkov, and I. L. Kharina, Protection of Metals (Russia), Vol. **24**, No. 6, 746, 1989.
7. J. Denk, 'Low pressure steam turbine integrity', Proc. Materials for Advanced Power Engineering, Liege, Belgium, 3-6 Oct, 1994, pp 157-170.
8. C. Lopez-Cacicedo and P. McIntyre, Stress Corrosion Cracking and Corrosion Fatigue of Blading Materials, Final Report on COST 501 Round II, WP 8 Project UK1, JCB 2302/003, 1992.
9. S. R. Holdsworth, Alstom, Private communication, 2001.
10. S. Zhou and A. Turnbull, 'Steam Turbines – Part I: Operating Conditions and Impurities in Condensates, Liquid Film and Deposit', Corrosion Engineering, Science and Technology, Vol. **38**, No.2, 97, 2003.
11. G. M. Sparkes, CEGB Report, MID/SSD/81/0015/R, 1981.
12. Deposition of Corrosive Salts from Steam, Palo Alto, CA, Electric Power Research Institute, April 1983, NP-3002.

13. Solubility of Corrosive Salts in Dry Steam, Palo Alto, CA, Electric Power Research Institute, June 1984, NP-3559.
14. O. Jonas, Steam Chemistry and Turbine Corrosion – State of Knowledge, Proc. Int. Water Conf., Palo Alto, CA, Vol. **54**, p. 297-310, 1993.
15. Corrosion of Steam Turbine Blading and Discs in the Phase Transition Zone, Palo Alto, CA, Electric Power Research Institute, November 1998, TR-111340.
16. O. Povarov, V. Semenov and A. Troitsky, Generation of Liquid Films and Corrosive Solutions on Blades and Discs of Turbine Stages, Specialist Workshop on Corrosion of Steam Turbine LP Blades and Discs, EPRI, February 9-11, 1998.
17. R. Ebara, T. Kai, M. Mihara, H. Kino, K. Katayama, and K. Shiota, Paper 4.10, p. 4-150, Ed, J. B. Marriott, Pub, Commission of the European Communities, ECSC-EEC-EAEC, Brussels, 1991.
18. R. Ebara, T. Yamada and H. Kawana, ISIJ International, Vol. **30**, No. 7, 535, 1990.
19. G. Gabetta and L. Torri, Fatigue Fract. Engng Mater. Struct., Vol. **15**, No.11, 1101, 1992.
20. M. Shalaby, J. A. Begley and D. D. Macdonald, Corrosion, Vol. **52**, No. 4, 262, 1996.
21. S. Zhou and A. Turnbull, Fatigue Fract. Engng Mater. Struct., Vol. **22**, No.11, 1083, 1999.
22. G. Williams and H. N. McMurray, Corrosion, Vol. **62**, No. 3, 231, 2006.
23. S. Zhou and A. Turnbull, Unpublished Report, November 2006.
24. A. Turnbull, Environment-assisted Fatigue in Liquid Environments, in Comprehensive Structure Integrity, Eds. I. Petit and P. Scott, Vol. **6**, p.163,Oxford (2003)
25. Kh-G, Schmitt-Thomas, W. G. Hauberberger und H. Meisel, Werkstoffe und Korrosion, Vol. **27**, 775, 1976.
26. M. H. EL Haddad, K. N. Smith and T. H. Topper, Fatigue crack propagation of short cracks, ASME Journal of Engineering Materials and Technology, **101**,42-46, (1979).
27. A. I. Lebedeva, V. S. Sokolov, V. F. Rezinskikh and A. F. Bogachev, Thermal Engineering, Vol. **39**, No. 2, p. 69, (1992).
28. S. Kawai and K. Kasai, Fatigue Fract. Engng Mater. Struct., Vol. **8**, No.2, 115, 1985.
29. E. Lachmann, Low Cycle Fatigue of Elastic-Plastic Behaviour of Materials, Munich, FRg, 7-11, September 1987, pp.348.
30. H. Yamannouchi, H. Kino and Ebara, Recent Investigations on Corrosion Fatigue Behaviour of 12Cr Stainless Steels For Steam Turbine Blades, ASTM 82-JPGC-PWR-18, 1982.
31. K. M. Perkins and M. R. Bache, International Journal of Fatigue, Vol. **27**, 1499, 2005.
32. A. Turnbull, W. Dietzel and A. J. Griffiths, Prenormalisation Research in Environment assisted cracking, Corrosion Standards II, p. 147, Eds. P. McIntyre and D. J. Mills, The Institute of Materials, London (1996).
33. H. Ishii, Y. Sakakibara and R. Ebara, Metallurgical Transactions A, **13A**, 1521, 1982.
34. S. Y. Cho, C. H. Kim and D. H. Bae, Key Engineering Materials Vol. **183-187**, 993, 2000.

35. A. Atrens, H. Meyer and K. Schneider, Steam Turbine Blades, Corrosion in Power Generation Equipment, Eds. M. O. Speidel and A. Atrens, 1984.
36. G. M. Sparkes, CEGB Report, MID/SSD/81/0055/R, 1981.
37. G. J. Seal and S. T. Rolfe, SERSSD, SSD/SE/R59/75, January 1976.